International Journal of Multiphase Flow 185 (2025) 105156

Contents lists available at ScienceDirect

International Journal of Multiphase Flow

journal homepage: www.elsevier.com/locate/ijmulflow

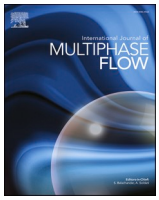

Research Paper

Breath of pollutants: How breathing patterns influence microplastic accumulation in the human lung

Hafiz Hamza Riaz [a,1], Abdul Haseeb Lodhi [a,1], Adnan Munir [b], Ming Zhao [b], Muhammad Hamza Ali [a], Emilie Sauret [c], YuanTong Gu [c], Mohammad S. Islam [d,*]

[a] School of Mechanical and Manufacturing Engineering, National University of Sciences and Technology, H-12, Islamabad, Pakistan
[b] School of Engineering, Design and Built Environment, Western Sydney University, Penrith, 2751, NSW, Australia
[c] School of Mechanical, Medical and Process Engineering, Faculty of Engineering, Queensland University of Technology, Brisbane, QLD 4000, Australia
[d] School of Mechanical and Mechatronic Engineering, University of Technology Sydney, Ultimo, NSW 2007, Australia

ARTICLE INFO

Keywords:
Human lung
Microplastics
Air pollution
Toxic particles
Respiratory diseases

ABSTRACT

Humans are likely exposed to indoor and outdoor microplastics due to increased plastic degradation processes in the last decade. When inhaled, these microplastics could lead to inflammatory and respiratory disorders. Recent studies have advanced our understanding of microplastic transport in the respiratory system; however, they often overlook the various breathing patterns, effects of particle shape and specific accumulation patterns in the tracheobronchial airways. This study uniquely investigates how microplastics of various shapes accumulate under different breathing flow rates and frequencies, providing new insights into their behavior within these critical airways. The key findings show that microplastic deposition is minimal at a low flow rate of 7.5 LPM and a cycle frequency of 0.5 Hz but increases significantly when the frequency drops to 0.25 Hz, especially in the main bronchus. Higher inhalation flow rates, such as 40 LPM, lead to greater microplastic deposition in the early generations of the tracheobronchial airways, including generations 1–8, with notable differences between the inhalation and exhalation phases. Smaller flow rates result in higher microplastic deposition in distal airways beyond generation 8. The risk of microplastic inhalation is higher in the right bronchi, with larger particles (4–10 μm) depositing more in the main bronchi at lower flow rates and smaller particles (1–3 μm) in the initial airways at higher flow rates. The findings of this study, including case-specific microplastic deposition hotspots, will contribute to the up-to-date knowledge on pollutant exposure and relevant preventive measures.

1. Introduction

Microplastics are plastic particles that have been produced continuously since mass production began and have penetrated the majority of life forms (Geyer et al., 2017). Initially, high concentrations of microplastics were found in marine life due to convenient routes available for microplastics to travel from land into water bodies via wind, littering, and direct or indirect dumping of industrial wastes near aquatic environments (Xu et al., 2020). Recently, notable concentrations of microplastics have been found in the air and these particles are now considered as one of the environmental pollutants (Xu et al., 2019). It is easy to apprehend that microplastics break into small units and can migrate from the environment to the human body through inhalation, ingestion, and food chain transfer (Amato-Lourenço et al., 2021, Jenner et al., 2022, Huang et al., 2022). Microplastics tend to deposit largely via inhalation and persist in the human lung airways for a long period (Yang et al., 2023). These particles, when introduced into the human sputum and respiratory tissue, can induce respiratory inflammation, oxidative stress, and cytotoxicity (Vethaak and Legler, 2021). Therefore, the possible adverse impacts of microplastics on the human respiratory system pose a risk to public health and suggest adequate research for a comprehensive understanding of microplastic exposure and migration within the human respiratory system.

The gas exchange phenomenon between the human body and the environment happens in the lung tissue of the respiratory system. This component is at risk of exposure to the harmful concentration of microplastics in the atmosphere. Numerous studies have been reported that have investigated and quantified particulate matter and

* Corresponding author.
E-mail address: mohammadsaidul.islam@uts.edu.au (M.S. Islam).
[1] The authors have contributed equally to this work

https://doi.org/10.1016/j.ijmultiphaseflow.2025.105156
Received 20 October 2024; Received in revised form 24 January 2025; Accepted 27 January 2025
Available online 28 January 2025

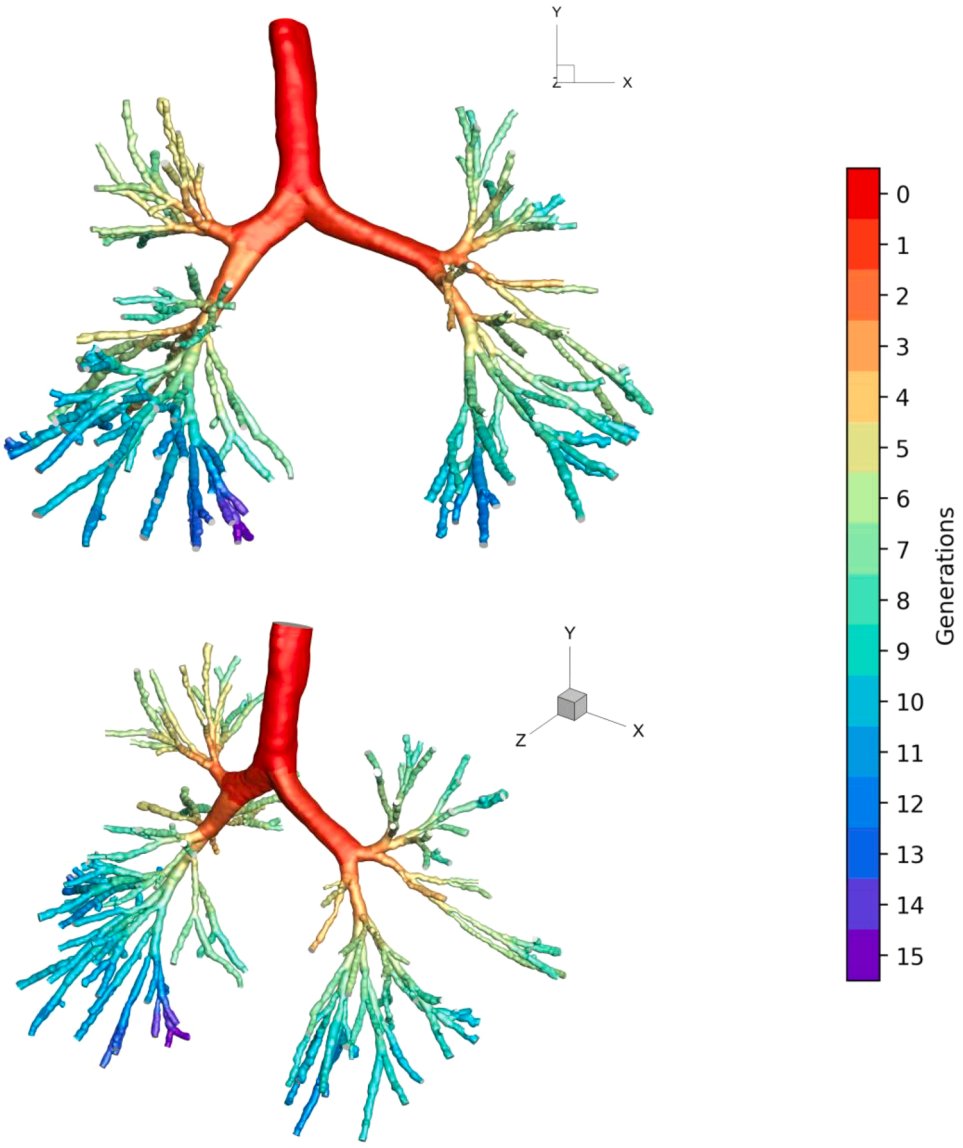

Fig. 1. Three dimensional CT-based respiratory lung model of a healthy adult.

microplastic particle concentrations in different environmental settings (Chithra and Nagendra, 2013, Ya et al., 2021). Some recent studies include investigations of bioaerosol inhalation and deposition in the different parts of the human respiratory system. Zuo et al. (2020), conducted a detailed review of existing studies on bio-aerosol transport in the context of airborne transmission of the SARS-CoV-2 virus. Wang et al. (2021) and Chong et al. (2021) studied the airborne virus transmission through respiratory droplets of various sizes, under different environmental (i.e., temperature, humidity) and respiratory conditions (i.e., breath, sneeze, puff). Haghnegahdar et al. (2019) advanced their investigation of droplets aerosol deposition to study the response of the immune system for both nasal and mouth-breathing scenarios. In addition to investigating health risks, studying aerosol transmission and deposition is important for medical solutions such as targeted drug delivery in the respiratory system (Heyder, 2004).

Particle deposition in the lungs happens through different primary mechanisms, influenced by particle diameter, airflow conditions, and respiratory physiology. Inertial impaction involves the process where large particles fail to follow the curvature of airflow due to their momentum, leading to deposition on airway surfaces. Gravitational sedimentation refers to the settling phenomenon of particles under the gravitational force, which becomes significant in slower airflow regions of the narrow airways (Chen et al., 2018). Brownian diffusion is another mechanism for particle deposition in the lung airways. This involves random movement of tiny particles ($< 1\ \mu m$) caused by collisions with gas molecules, leading to their deposition in the peripheral and deeper generations of the lungs (Rahman et al., 2022). Compared to in-vivo or in-vitro experiments, numerical simulations have shown effectiveness in predicting the trajectories of inhaled particles. This method avoids risks to human subjects and aids physicians in understanding the impact of deposited particles. Many experts have employed computational fluid dynamics techniques to investigate the behavior of inhaled aerosols of different natures (Khoa et al., 2023, Rahman et al., 2021a, Islam et al., 2021). The existing studies on aerosol transport in lungs have reported their findings for different inhalation and environmental conditions but mainly for spherical particle shape (Rahman et al., 2021b, Khoa et al., 2023). The research on deposition patterns of non-spherical particles, such as microplastics, in the human respiratory tract is still in its early stages, with only a few available studies in the literature. There are many studies on the flow dynamics of non-spherical particles, but not specifically focused on the human respiratory system. Voth and Soldati (2017) reviewed recent studies on anisotropic particles which are not

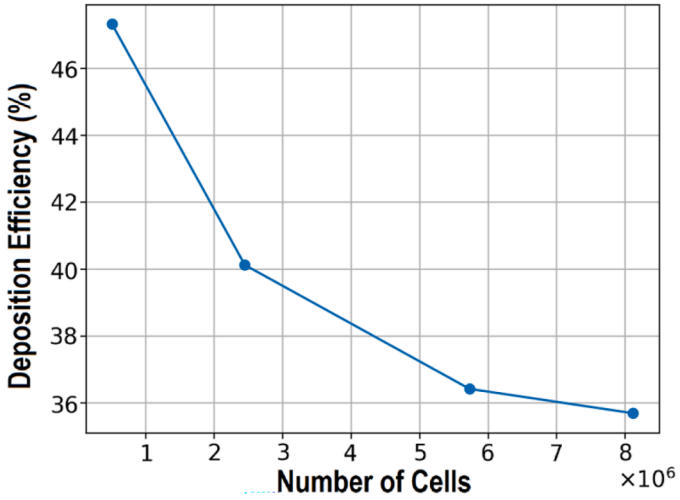

Fig. 2. Variation of deposition efficiency of particles in the tracheobronchial airways with the mesh elements at 40 LPM and breathing frequency of 0.5 Hz.

neutrally buoyant and presented their behaviour under turbulent flow conditions. Marcus et al. (2014) studied the orientation and rotation of ellipse-, disk- and sphere-shaped particles over a range of aspect ratio. Overall, the particle shape is found to have a significant effect on flow dynamics and drag in turbulent flows (Soldati and Marchioli, 2009, Marchioli et al., 2010, Do-Quang et al., 2014).

For the human lungs, Jia et al. (2018) studied the deposition of microplastics with different shape factors in the upper respiratory tract of a realistic model and found a close relation between the deposition fraction and particle shape factor. Islam et al. (2023) first investigated the movement and deposition of non-spherical particles in the upper human airways including nasal cavities, mouth-throat, pharynx, epiglottis, and trachea. They reported higher deposition efficiency of microplastics at lower flow rate in the upper airways. They also found that particles with spherical and tetrahedral shapes have similar deposition efficiency which was lower than cylindrical particles at the flow rate of 7.5 LPM. In the latest study, Riaz et al. (2024) simulated multiple non-spherical microplastic shapes and investigated their migration and deposition in the realistic human tracheobronical airways from the trachea to 5th generation of the lung airways. Their primary findings indicated varying deposition hotspots of microplastic particles at different inhalation flow rates. The deposition of non-spherical drug particles with tomahawk shape was studied by Tanprasert et al. (2023). They used an idealistic human airway model extending from G0 to G5 and reported that tomahawk-shaped particles were deposited more conveniently as compared to the cylindrical drug particle shape. Recently, Huang et al. (2024) presented their findings on the transport and deposition of nano and microplastics in the human respiratory system. Their investigation utilized the realistic CT-based human airway model from the nasal cavity to the 13th generation of the bronchial tree. A comparison between the deposition patterns of nano and microplastic particles was demonstrated in which the microplastics were reported to be deposited significantly at slower breathing rates, particularly within the nasal cavity and larynx.

The comprehensive literature review reveals significant knowledge gaps, including (a) understanding the transport behavior of microplastic particles in the tracheobronical tree of the human respiratory system under realistic breathing conditions; (b) investigating the potential exposure and microplastic mass deposition in the human respiratory airways from trachea to the deeper lung generations; and (c) accessing the impact of inhalation flow rates, particle size, and particle geometry on the flow dynamics. The current work aims to bridge these gaps by achieving the objectives: (1) design and validate the numerical model to simulate the non-spherical microplastic particles in the realistic human tracheobronical tree under different inhalation conditions, (2) to determine the relationship between the inhalable microplastic particle size, shape, and flow conditions on the microplastics transport, (3) to calculate the mass deposition of microplastic particles, and (4) to predict the risk contribution levels of microplastic particles for different lung regions.

The current work targets to improve the understanding of the flow dynamics of microplastic particles and airflow in the complex bifurcating human respiratory airways, thereby facilitating optimized and effective pollutant prevention and inhalation treatments. This study employs a computational fluid dynamics-based discrete phase modelling technique to investigate pollutant particles migration and deposition under realistic breathing conditions.

2. Airway model

The respiratory model of the airways network is obtained using the CT-based DiCom images of a healthy adult. The three-dimensional model includes trachea pipe and bifurcating generations up to G15, 1 inlet face, and 167 outlet faces with left lower lobe, left upper lobe, right lower lobe, right middle lobe, and right upper lobe consisting of 44, 28, 52, 22, and 21 outlets respectively, as illustrated in Fig. 1. ANSYS meshing is used to generate an unstructured mesh of the lung model. The optimal number of grid elements is selected based on the mesh independency criteria shown in Fig. 2. A total of four polyhedral meshes in the range of 0.5-9 million grid elements with 10 inflation layers are studied, and the variation in the deposition efficiency of spherical particles between each mesh is calculated. The final mesh, shown in Fig. 3, with grid elements equal to 5.7 million, is chosen for the formal investigation of the migration of microplastic particles in the human lung airways.

3. Methodology

The numerical model is designed in ANSYS Fluent software to simulate the microplastic pollutant particles in the human respiratory airways tree. The air flow fields in human lungs are accurately predicted by solving the Reynolds-averaged Navier–Stokes equations (Arsalanloo et al., 2022):

$$\nabla\cdot\mathbf{u} = 0, \tag{1}$$

$$\frac{\partial \mathbf{u}}{\partial t} + \nabla\cdot(\mathbf{u}\mathbf{u}) = -\frac{1}{\rho}\nabla p + \nu\nabla^2\mathbf{u} - \nabla\cdot\boldsymbol{\tau} \tag{2}$$

here $\mathbf{u}$, ρ, p, ν, and $\boldsymbol{\tau}$ are fluid velocity, fluid density, static pressure, kinematic viscosity of the fluid, and Reynolds stress tensor, respectively. The $k-\omega$ shear stress transport (SST) turbulence model is employed for the accurate calculations of pressure gradients near the airway walls. The $k-\omega$ SST model enhances the standard $k-\omega$ model by effectively combining accurate near-wall treatment with the ability to maintain free-stream independence in the far-field region. The turbulent kinetic energy (k) and dissipation rate (ω) are predicted using:

$$\frac{\partial(\rho k)}{\partial t} + \nabla\cdot(\rho\mathbf{u}k) = \nabla\cdot(\Gamma_k\nabla k) + \widetilde{G}_k - Y_k, \tag{3}$$

$$\frac{\partial(\rho\omega)}{\partial t} + \nabla\cdot(\rho\mathbf{u}\omega) = \nabla\cdot(\Gamma_\omega\nabla\omega) + \widetilde{G}_\omega - Y_\omega \tag{4}$$

The turbulence model mixes and transfers k and ω using effective diffusivity terms (Γ_k and Γ_ω). G represents the generation term and Y is the dissipation term of turbulence. To simulate the motion of the microplastic particles in the Lagrangian scheme and airflow in the Eulerian scheme, the one-way coupling Discrete Phase Model (DPM) is employed with implicit formulation. This model facilitates particle tracking in the airway tree under various settings. This approach is particularly advantageous for investigating localized deposition trends

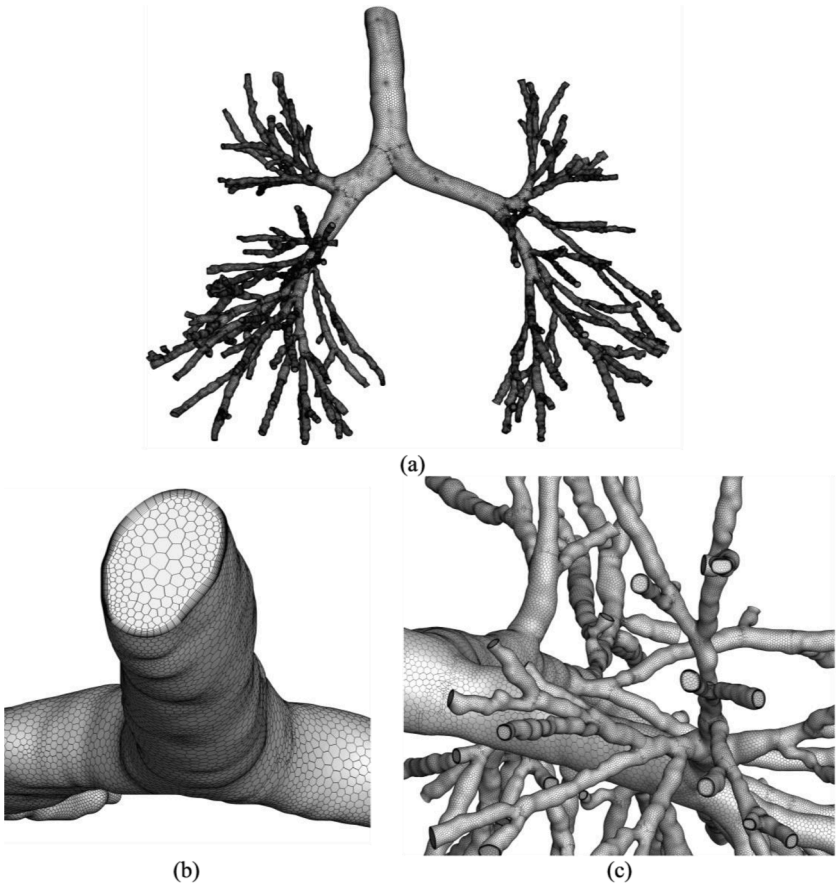

Fig. 3. (a) Polyhedral mesh of the tracheobronchial airways; (b) Inlet face mesh; (c) Outlet faces mesh with inflation layers.

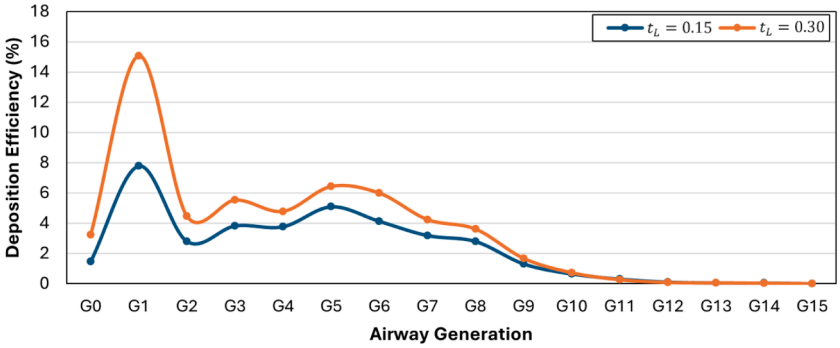

Fig. 4. Sensitivity of the model to the time scale constant parameter.

within the complex geometry of the airway tree during both inhalation and exhalation phases. A pressure–velocity coupling scheme and 2nd order discretization technique is used for the spatial discretization of momentum, volume fraction, and turbulent kinetic energy. Discrete random walk model that employs the random eddy lifetime approach is enabled for modelling the turbulent dispersion of the inhaled microplastic particles. The integral time scale constant (t_L), which governs the interaction time between particles and turbulent eddies and directly impacts particle deposition predictions, is carefully selected through validation against experimental and numerical data. Fig. 4 shows the deposition efficiency values for spherical particles across various airway generations for different t_L values, highlighting the model's sensitivity to this parameter. A higher time scale constant enhances particle dispersion by prolonging interaction with larger turbulent eddies, leading to overpredicted particle deposition in turbulence-intense regions like G1, where secondary flows dominate. In the current study, a time scale constant of 0.15 is chosen, as it provides deposition predictions close to the available experimental and numerical results. The discrete random walk model tracks microplastic particle movement in lung airways by simulating particle motion in discrete time steps and spatial increments. At each step, a particle moves to a new position based on predefined probabilities, accounting for factors such as airway structure, airflow direction, and deposition mechanisms.

The realistic breathing profile has a longer exhalation period than inhalation. However, Gupta et al. (2010) demonstrated that a sinusoidal wave can adequately represent the normal breathing profile. Hence, a sinusoidal breathing profile with a period of 2 s (Inthavong et al., 2010), illustrated in Fig. 5, is employed at the inlet tracheal face to simulate realistic breathing conditions at different pulsating inhalation flow rates ($\dot{Q}_0$) e.g., 7.5, 15, and 40 LPM (litres per minute). Additionally, for 7.5

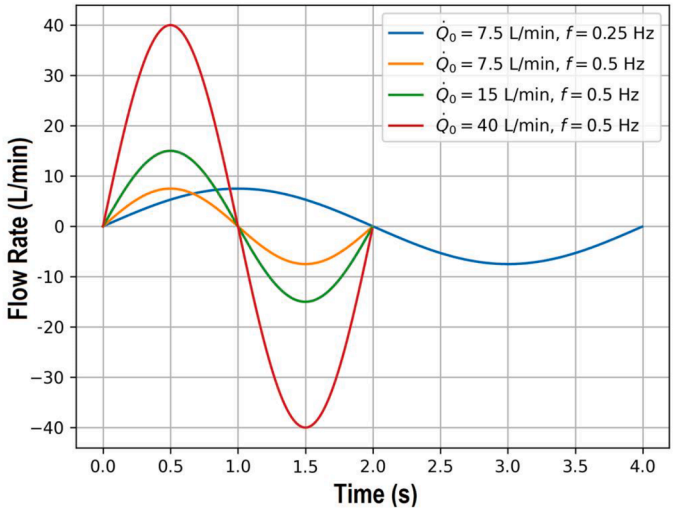

Fig. 5. Velocity profiles for different inhalation flow rates.

LPM, a breathing profile of 4 s period is also used to investigate the effect of different breathing cycle frequencies on the microplastic particles deposition. The selected flow and breathing frequencies reflect a range of physiological conditions (Ciloglu, 2020), from normal tidal breathing to elevated rates during respiratory distress. These values correspond to typical respiratory patterns in both healthy individuals and those with conditions like asthma or COPD (Inoue et al., 1997), emphasizing the relevance of the findings to real-world scenarios. At the outlets, a zero-gauge pressure condition is applied (Jing et al., 2023). The lung walls are assumed to be rigid and stationary with a no-slip condition. For tracking the deposited microplastic particles, a trap condition is applied at the lung walls. Given the stickiness of mucus on airway walls, the trap condition is a reasonable approximation. This is a common practice in studies emphasizing the particle deposition trends in lung airway tree, as it simplifies the interactions between the inhaled particles and airway walls (Rahman et al., 2024, Khoa et al., 2023, Gou et al., 2024). The trap condition registers a particle as trapped upon reaching the airway wall, removing it from the domain and preventing any further interaction.

The movement of the discrete phase particle (microplastic) is simulated through the integration of differential equation for the microplastic force equilibrium:

$$m_p \frac{d\boldsymbol{u_p}}{dt} = \frac{1}{8}\pi\rho d_p^2 C_D(\mathbf{u}-\mathbf{u_p})|\mathbf{u}-\mathbf{u_p}| + m_p\mathbf{g} + \mathrm{F_L} \tag{5}$$

The above equilibrium equation is governed by mass of the microplastic particle (m_p), velocity of the particle ($\boldsymbol{u_p}$), drag force with C_D as coefficient of drag, d_p as microplastic particle diameter, gravitational force ($\mathbf{g}$), and Saffman lift force ($\mathrm{F_L}$). The density of the microplastic particle (ρ_p) is set at 940 kg/m^3. The dominant size of the microplastic particles discovered in the human lung tissues is in the micrometre range according to a study by Amato-Lourenço et al. (2021). Therefore, the current study simulates microplastic particles in the size range of 1-10 μm.

For modelling different non-spherical shapes of microplastic particles, the shape factor and sphericity concept are employed. The shape factor ($\varnothing$) is the ratio of the surface area of sphere (A_s) having the same volume as that of the particle and the actual surface area of the particle (A_p) (Wadell, 1934):

$$\varnothing = \frac{A_s}{A_p} \tag{6}$$

The expression in Eq. 6 is employed to calculate the shape factors for different particle shapes such as cylindrical, cube, and tetrahedral. Various shapes and sizes of microplastic particles are injected into the tracheal inlet face at once. A polydisperse injection is used where a total of 60,000 particles for each shape and 6000 particles for each diameter in the range of 1–10 μm are introduced in the domain. Haider and Levenspiel (1989) reported the calculation of drag coefficients for different shapes of particles as:

$$C_{D_{\text{spherical}}} = \frac{24}{Re_{sph}} \tag{7}$$

$$C_{D_{\text{non-spherical}}} = \frac{24}{Re_{sph}}\left(1 + a_1 Re_{sph}^{a_2}\right) + \frac{a_3}{1 + \frac{a_4}{Re_{sph}}} \tag{8}$$

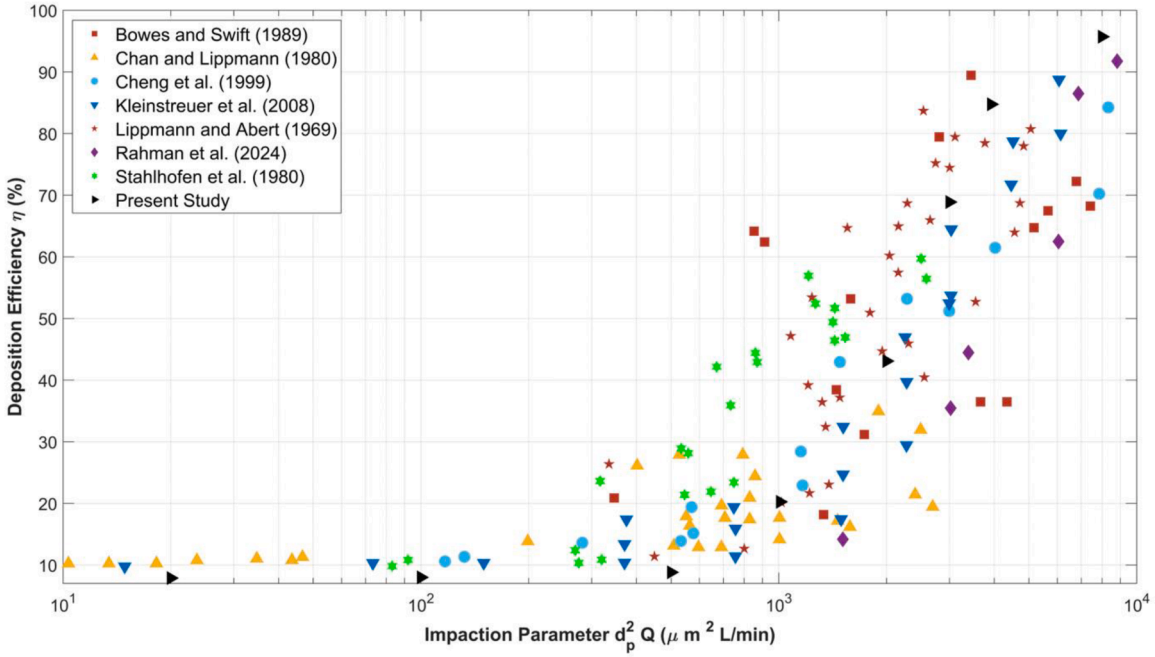

Fig. 6. Model validation: Comparison of deposition of microparticles in the mouth–throat region between the current study and published research against the impaction parameter.

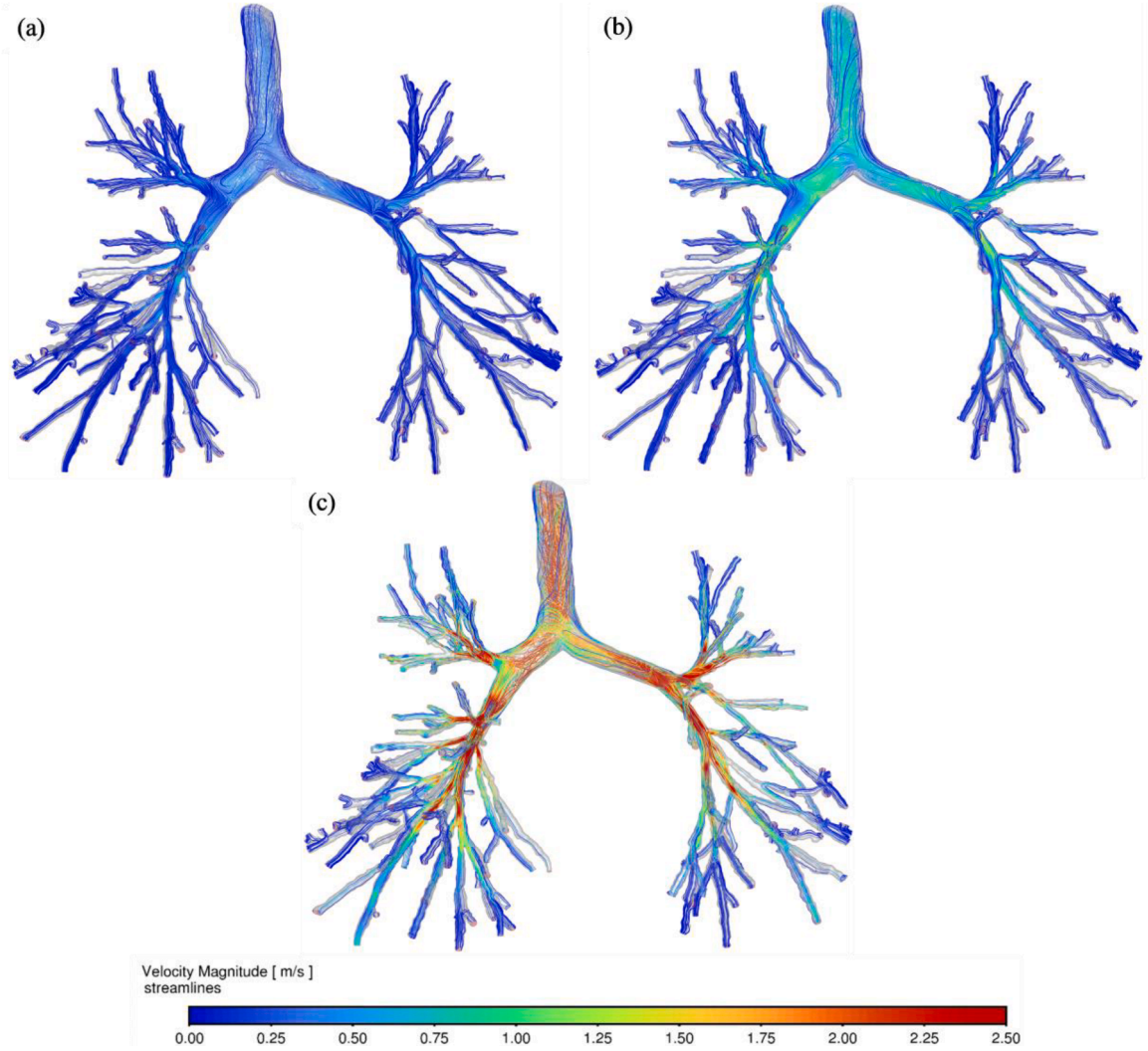

Fig. 7. Velocity streamline contours in the lung airways for the inhalation flow rate of (a) 7.5 LPM; (b) 15 LPM; (c) 40 LPM.

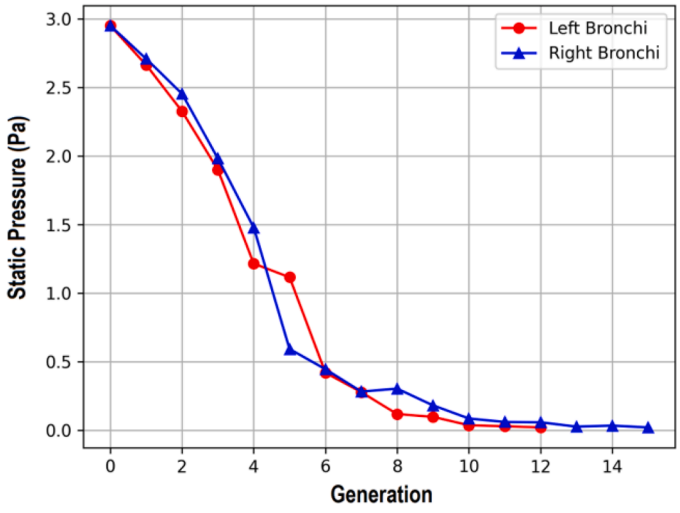

Fig. 8. Static pressure values for each lung airways generation at the flow rate of 15 LPM.

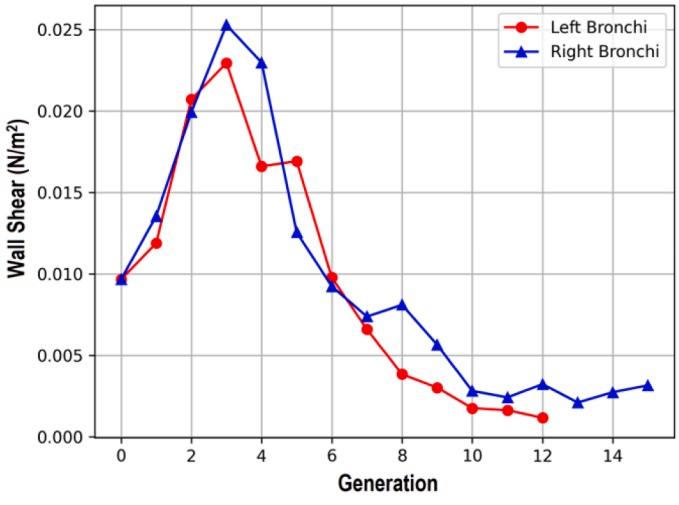

Fig. 9. Wall shear values for each lung airways generation at the flow rate of 15 LPM.

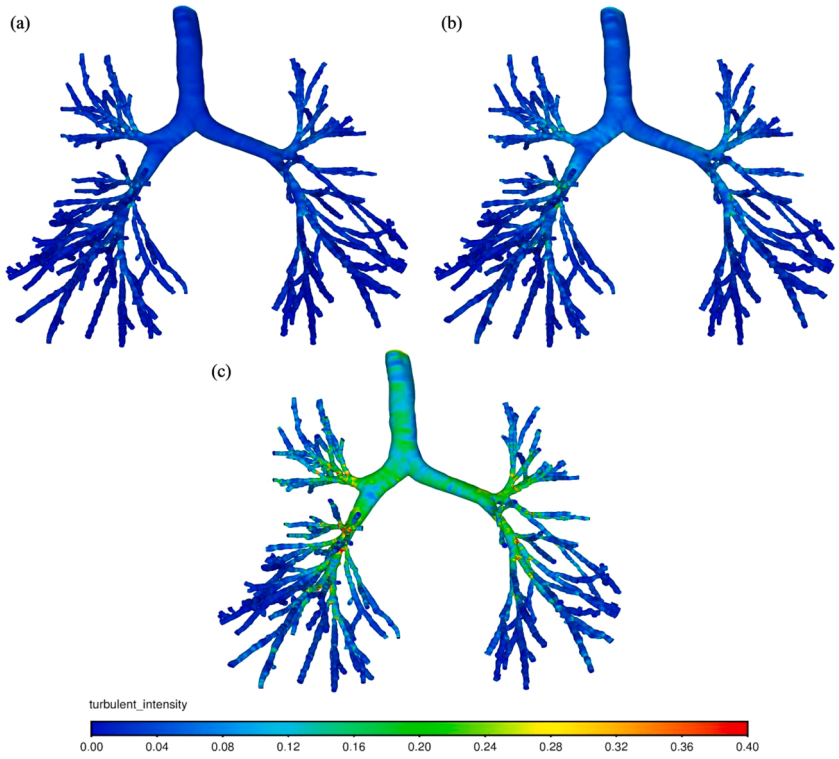

Fig. 10. Turbulent intensity contours in the lung airways for the inhalation flow rate of (a) 7.5 LPM; (b) 15 LPM; and (c) 40 LPM.

where Re_{sph} is the Reynolds number for spherical microplastic particle. The constants in Eq. 8 are based on the shape factor value of each particle shape:

$$\left.\begin{array}{c} a_1 = e^{\left(2.3288-6.4581\varnothing+2.4486\varnothing^2\right)}, \\ a_2 = e^{\left(0.0964+0.5565?\right)}, \\ a_3 = e^{\left(4.905-13.8944\varnothing+18.4222\varnothing^2-10.2599\varnothing^3\right)}, \\ a_4 = e^{\left(1.4681+12.2584\varnothing-20.7322\varnothing^2+15.8855\varnothing^3\right)} \end{array}\right\} \quad (9)$$

Various non-dimensional parameters characterize the behavior of microplastic particles in the airflow. The bulk Reynolds number quantifies the relative importance of inertial forces to viscous forces in the flow of the fluid. The Reynolds number of the spherical microplastic particle defines the flow regime around an individual particle, considering its diameter and velocity relative to the surrounding fluid. It is given by:

$$Re_{sph} = \frac{\rho d_p |\mathbf{u} - \mathbf{u_p}|}{\mu} \quad (10)$$

where d_p is the diameter of the microplastic particle. Another term that controls the particle behavior is the Stokes Number (Stk), and it is used to describe the particle's ability to follow the fluid flow. It is defined as:

$$\text{Stk} = \frac{\rho_p d_p^2 \mathbf{u}}{18\mu D} \quad (11)$$

The diameter of the inlet face of the trachea is represented by D here.

In the study, microplastic particles in the tracheobronchial tree are either trapped on the airway walls or escaped from the outlets to the smaller airways. The current research assumes that all trapped microplastic particles contribute to inducing tissue inflammation and lung cancer at the deposited sites. For this, the following risk contribution fraction (RCF) is used to assess the carcinogenic potential in each lung bronchi:

$$RCF\ (\%) = \frac{N_d + N_e}{N_i} \times\ 100 \quad (12)$$

where N_d and N_e are the number of particles deposited and escaped from a particular bronchus region respectively and N_i is the total number of particles inhaled in the lung airways.

The computational model employed in the current study has been validated for accurate prediction of microplastic particle transportation in the respiratory system. Experimental and numerical data on the deposition rate of particles in the mouth-throat section of the human respiratory system is used for validating the current model. Fig. 6 shows the comparison of deposition efficiency between current and existing studies (Bowes III and Swift, 1989, Chan and Lippmann, 1980, Cheng et al., 1999, Kleinstreuer et al., 2008, Lippmann and Albert, 1969, Stahlhofen et al., 1980, Rahman et al., 2024) in the literature for particles in micrometre scale against the impaction parameter (d_p^2Q). The trend shown in Fig. 6 indicates the accuracy of current model for the investigation of particle flow patterns.

4. Results and Discussion

4.1. Airflow Dynamics

The investigation of microplastic migration in the human respiratory system is conducted at various inhalation flow conditions. The impact of such flow conditions on the velocity profile is illustrated in Fig. 7. Between the three inlet flow rates, the flow profile is more complicated at 40 LPM inhalation conditions. Generation of secondary vortices is observed at the bifurcating sections of the tracheobronchial tree for the high inhalation flow rate. The laminar streamlines at lower inhalation flow rate disperse almost evenly within the complete airways network. As the inhalation flow rate increases, the magnitude of the velocity streamlines strengthens for the proximal generations of the airways tree. The right bronchi being wider allows for more flow rate and volume. The initial airways in the tree such as generations G1-G7 experience comparatively higher velocity magnitudes than the large trachea. For deeper and narrower generations like G10-G15, the velocity magnitude drops because of the branching effect and increased total cross-sectional

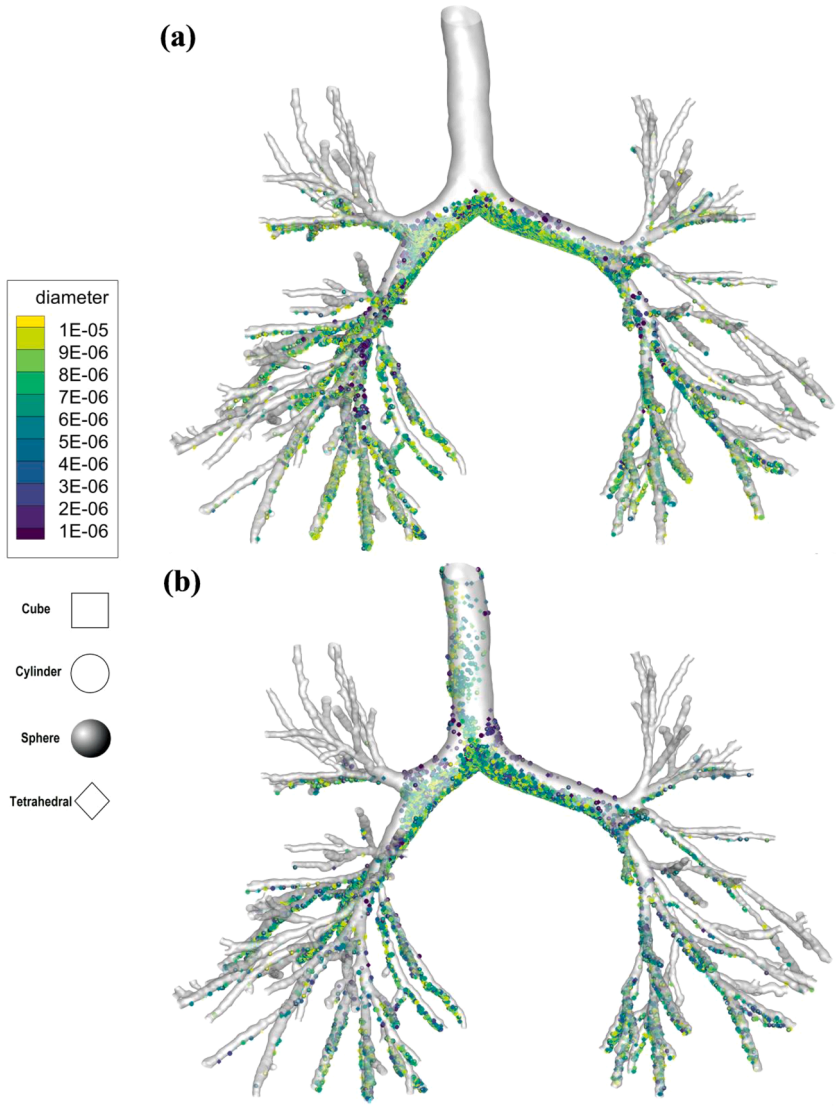

Fig. 11. Local microplastic deposition during (a): inhalation and (b): exhalation in human tracheobronchial airways with particle size 1–10 μm at inhalation flow rate of 7.5 LPM and breathing frequency of 0.25 Hz.

area compared to the proximal generations. This observation holds for each inhalation flow rate.

As the air moves through the airways of a tree, the sizes of branches reduce but their number increase significantly, resulting in increased total cross-sectional area after every generation. After each generation, the increased total cross-sectional area of all the airways results in a reduced velocity and consequently reduced resistance of the wall shear on the flow. As a result, the pressure drops slower after each generation as shown in Fig. 8 that shows the value of static pressure for both the left and right bronchi of the human lung at the inhalation flow rate of 15 LPM. Since pressure is being driven by the larger, proximal airways, there is an overall decrease in pressure as air moves to the more distal regions. In the larger airways like the trachea and main bronchi, in addition to the high velocity shown in Fig. 7, the flow is highly turbulent compared to the distal and smaller airways. Hence, a high-pressure loss is found for the initial generations and low-pressure loss happens in smaller airways where the flow is laminar.

The strong turbulence with high airflow velocities in the large trachea and main bronchi lead to increased shear stress on the airway walls. Fig. 9 illustrates the wall shear values for all the airway generations at the inhalation flow rate of 15 LPM. As the air moves from the trachea to smaller branches up to G3, the overall flow rate remains high. Moreover, the reduction in the airway diameter from the trachea to G3 enhances the airflow velocity. All these factors cause an increase in wall shear as the air flows from G0 to G3. Beyond G3, increased number of airway branches after every generation contributes to an increase in total cross-sectional area, a decrease in airflow velocity, and a reduction in the wall shear. Furthermore, the laminar nature of flow in the distal and smaller airways also plays a part in lower wall shear values.

Turbulent intensity indicates the degree of chaotic, irregular flow of air within the airways, characterized by fluctuations in velocity and pressure. It is a measure of the turbulent kinetic energy relative to the mean flow, and it affects how efficiently air is transported and distributed through the respiratory system. The turbulent intensity contours for different inhalation flow rates are illustrated in Fig. 10. The high flow turbulence in the larger airways and subsequent development of secondary vortices contribute to increased turbulent intensity for the trachea and initial generations at a larger inhalation flow rate. The bifurcation points in these airways experience maximum turbulent intensity due to the abrupt and sharp changes in the flow path and speed. The flow separation combined with varying cross-sectional area generated regions of higher turbulence intensity especially at the bifurcation regions of G2-G4 in the upper and right middle lung lobes and G2-G7 in the lower lung lobes. The turbulent intensity eventually plays a

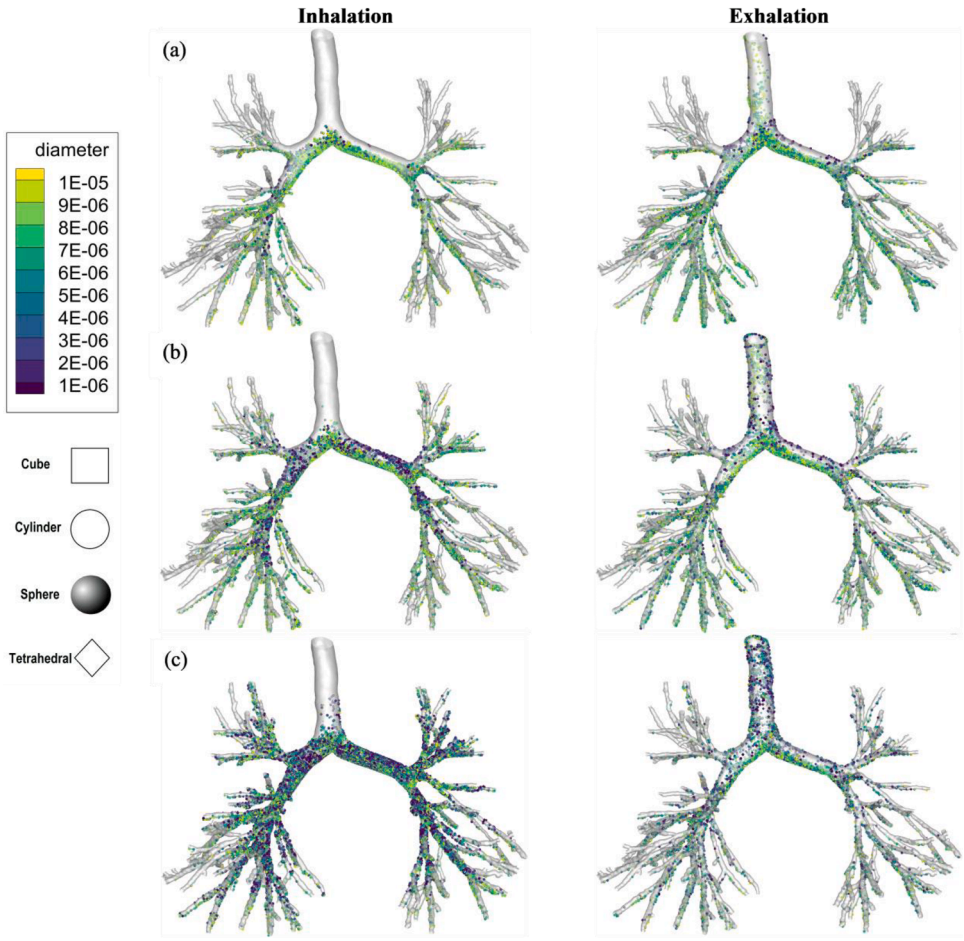

Fig. 12. Local microplastic deposition during inhalation and exhalation in human tracheobronchial airways with particle size 1–10 μm at inhalation flow rate of (a): 7.5 LPM; (b): 15 LPM; and (c) 40 LPM and breathing frequency of 0.5 Hz.

significant role in determining the deposition sites for inhaled particles in the lung airways.

4.2. Microplastic Particle Dynamics

The deposition of microplastic particles in the tracheobronchial airways with sizes ranging from 1-10 μm and four shapes is visualized in Fig. 11 for the flow rate of 7.5 LPM and 0.25 Hz frequency. Microplastic particles deposition during both inhalation and exhalation phase of the breathing cycle is shown separately in Fig. 11 (a) and (b), respectively. For comparison between different flow rates, Fig. 12 illustrates the local microplastic deposition for all other flow rates studied. The minimum microplastic deposition is shown for the smallest inhalation flow rate of 7.5 LPM with a breathing frequency of 0.5 Hz. In contrast, a flow rate of 40 LPM shows the highest deposited microplastic particles of all shapes and sizes during both the inhalation and exhalation phases. During inhalation, negligible microplastic deposition is observed in the trachea due to its larger size and laminar flow nature even at the flow rate of 40 LPM. It is during exhalation that particles are deposited in the trachea since flow is already fully developed and has high turbulence coming from distal and smaller airways back to the trachea. Moreover, it is also found that at a lower flow rate of 7.5 LPM for both 0.25 and 0.5 Hz frequency, the inhaled microplastic particles with size greater than 5 μm are deposited in the main bronchi and proximal airways. The smaller particles move towards the distal airways and either deposit there or escape towards alveolar sacs. At high flow rates, the particles with sizes 1-5 μm start to deposit in the main bronchi and proximal airways.

Fig. 13 illustrates the deposition of different shapes of microplastic particles during the complete breathing cycle at the flow rate of 7.5 LPM and 40 LPM. These deposition figures indicate that at lower flow rate, microplastic particles are deposited mainly in proximal airways which are towards the centre of the airway tree. Furthermore, in such airways, particles are dominantly deposited at the inner walls near the bifurcating points. This can be due to reduced velocity and increased residence time at lower flow rates which causes laminar airflow in the central airways as compared to the peripheral ones. At a larger flow rate of 40 LPM, particles deposit more evenly at the inner and outer curves of the airways. The high inertial impaction at this flow rate causes the microplastic particles to deposit at the airway wall especially when there is a sudden change in the flow direction or airway diameter. This is more pronounced for central airways due to larger diameters and changes in the flow direction.

A comparison of total deposition efficiencies of microplastics obtained for each airway generation in left and right bronchi between different inhalation flow rates is shown in Fig. 14. Even though the overall deposition efficiency in the tracheobronchial airways is highest for the larger flow rate of 40 LPM, the trend is a little different when considering the individual airway generations. In the earlier generations including trachea, main bronchi, and up to G8, the maximum deposition is found for 40 LPM in both left and right bronchi. There is an exception of the right bronchi of G6 for this observation. For G9-G15, smaller flow rates dominate the maximum microplastic particle deposition. At a flow rate of 40 LPM, the deposition rate increases by 15.9 % in generations G1–G8 compared to 15 LPM. However, in generations G9–G15, the deposition rate decreases by 0.6 % at 40 LPM relative to 15 LPM. The high inertial impaction at a larger flow rate combined with high

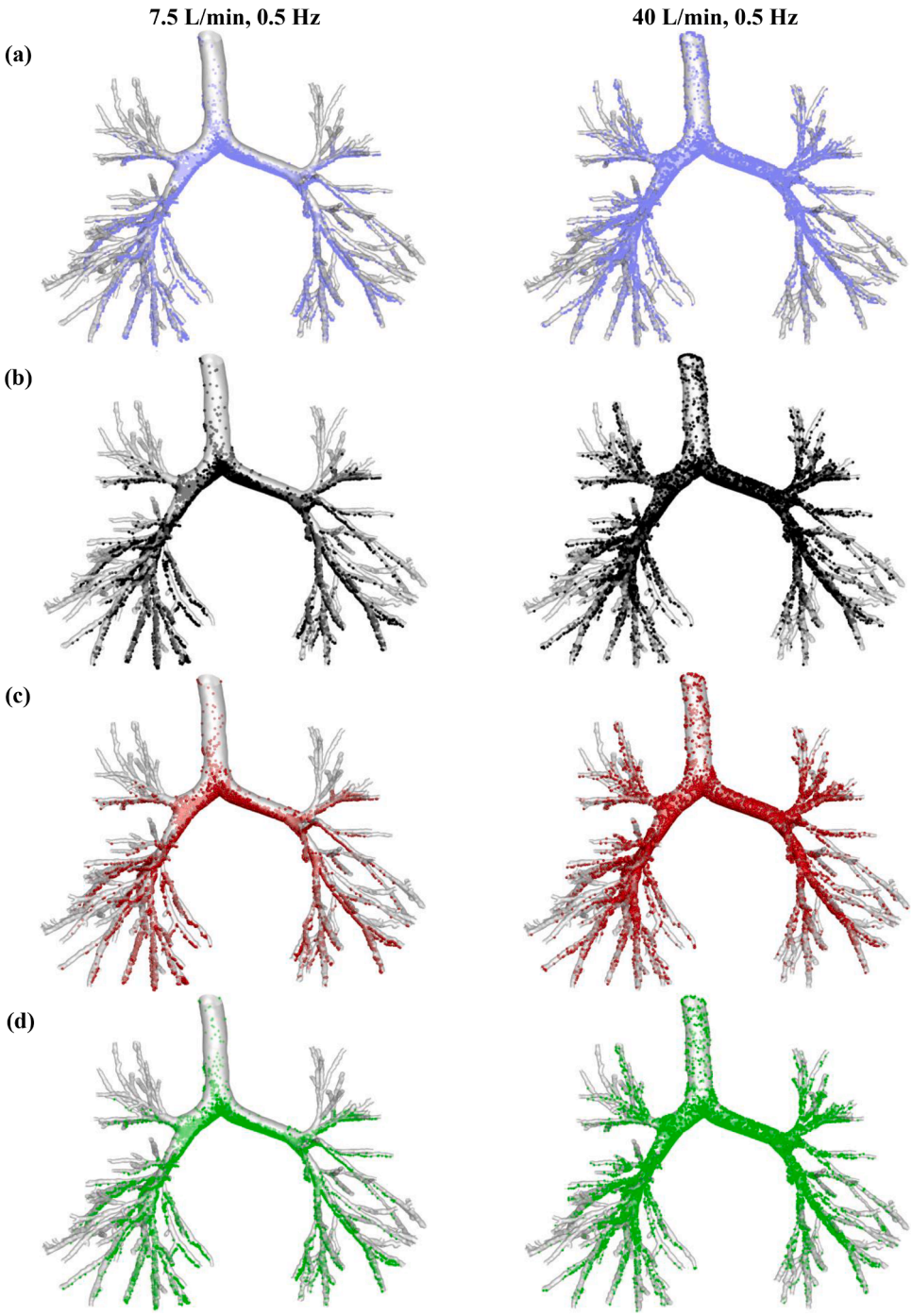

Fig. 13. Local microplastic deposition in human tracheobronchial airways at inhalation flow rate of 7.5 LPM, 0.5 Hz and 40 LPM, 0.5 Hz for shape (a): Cube; (b): Cylinder; (c): Sphere; and (d): Tetrahedral.

turbulence causes the particles to deposit early and more in the proximal airways and less in the distal airways.

The deposition efficiency is highest for right generations of the airway tree except for the G1 and G3. This is due to the wider size of right main bronchi and inclination of airflow towards right bronchi due to its more vertical orientation. In Fig. 14, when looking at the different breathing cycle frequencies for 7.5 LPM flow rate, it is found that reducing the frequency to 0.25 Hz or increasing the period of the breathing cycle to 4 seconds leads to higher microplastic deposition in the airways tree as compared to the 0.5 Hz frequency or 2 s period. This is because the low frequency at 7.5 LPM allows the microplastic particles to have a longer residence time and therefore, have a high probability to deposit in the airways. Hence, a higher deposition rate is found for a lower frequency of 7.5 LPM flow rate in multiple airway generations including trachea, right branches of G1-G7 and both branches of G9-G15.

The role of breathing phases on the microplastic deposition in the left and right bronchi is shown in Fig. 15 for the flow rate of 40 LPM. The overall microplastic deposition is higher during the inhalation phase as compared to the exhalation phase in both bronchi. During inhalation, the airflow is faster and more turbulent as it moves into the airways. This enhances the inertial impaction for the microplastic particles, and they do not follow the airstream smoothly and are more susceptible to colliding and trapping at the airway walls. Furthermore, the impact of

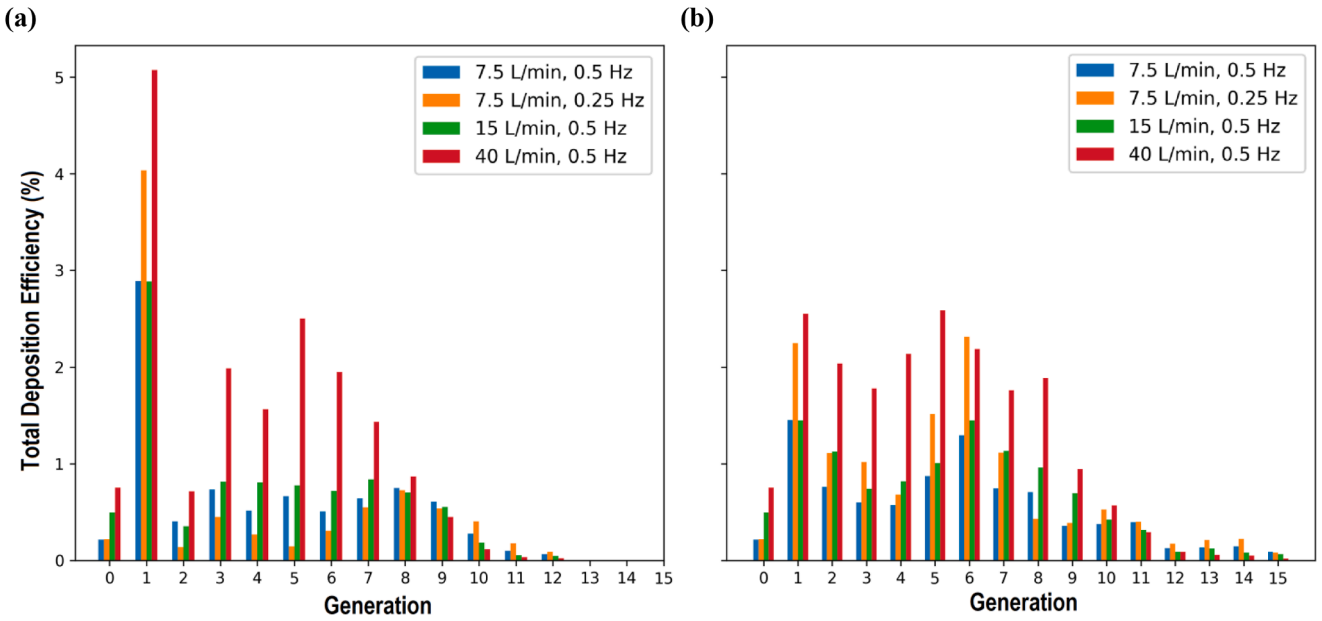

Fig. 14. Total deposition efficiency of microplastic particles in each generation of the airways for different inhalation flow rates in (a): left bronchi, and (b): right bronchi.

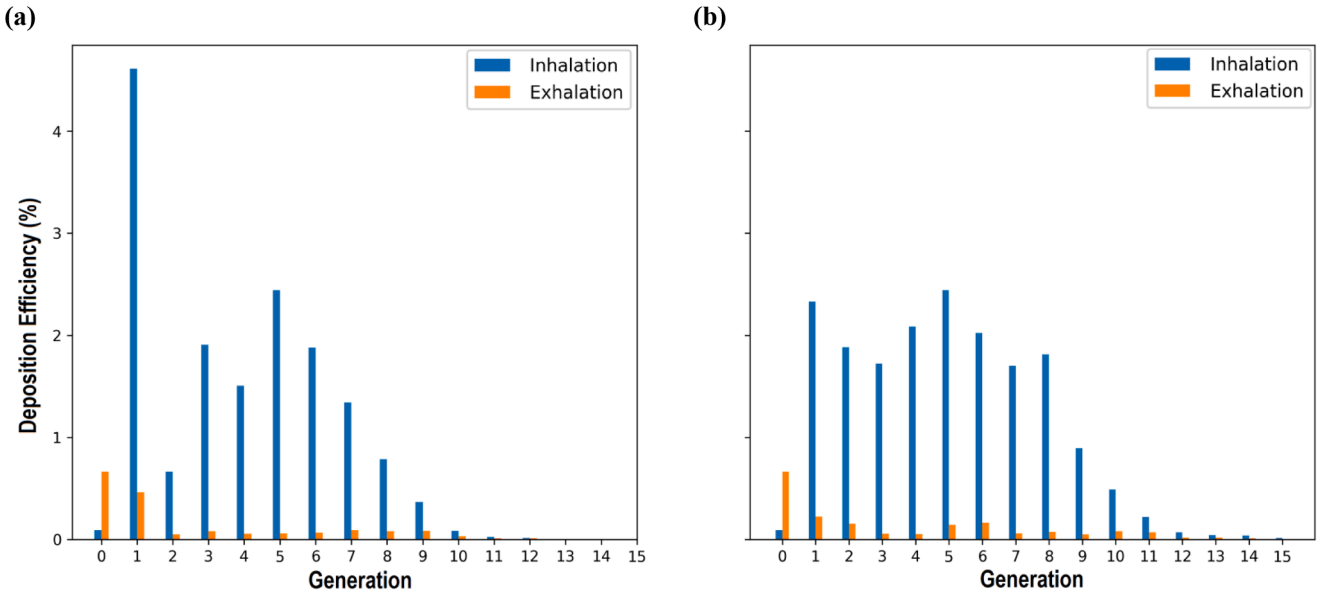

Fig. 15. Deposition efficiency of microplastic particles in left and right bronchi during inhalation and exhalation at 40 LPM in (a): left bronchi, and (b): right bronchi.

gravitational sedimentation plays a significant role in the higher microplastic deposition during the inhalation phase particularly for smaller airways. During exhalation, the airflow is usually slower and laminar, which makes the particle deposition in the distal airways negligible. The clearance mechanisms of the airways indicate that when microplastic particles are trapped or penetrated in the lung tissues, they can adhere to the airway walls and are not cleared during exhalation easily. The forceful expulsion of air carries some in-fluid microplastic particles out of the lower airways and deposits them in the initial generations such as G0-G6.

The impact of microplastic particle size on their penetration in the lung airways is illustrated in Fig. 16. Due to the flow inclination and more vertical orientation, the majority of the microplastic particles flow towards the right branch and each size of the microplastic particle ranging from 1–10 μm deposits more in the right bronchi. As the inhaled particle size increases, more particles are deposited due to higher inertial impaction. As the highest inhalation flow rate reports maximum microplastic deposition, the risk contribution fractions are calculated at 40 LPM. Fig. 17 shows the risk contribution fraction associated with microplastic inhalation against varying particle diameters and Stokes number. In Fig. 17(a), at first, the risk contribution fraction is higher for a smaller particle size of 1 μm for both right and left bronchi. It starts to decrease for 2–4 μm in the left bronchi and 3-4 μm in the right bronchi. As the particle diameter increases beyond 4 μm, the risk contribution fraction goes up smoothly with the peak value of 43.06 % and 35.59 % in the right and left bronchi respectively for the particle size of 10 μm. This plot suggests that larger microplastic particles could induce a higher probability of health hazards. The risk contribution fraction of right bronchi is, on average, 20.8 % more due to large flow inclination. The Stokes number is a dimensionless quantity based on the inlet diameter of

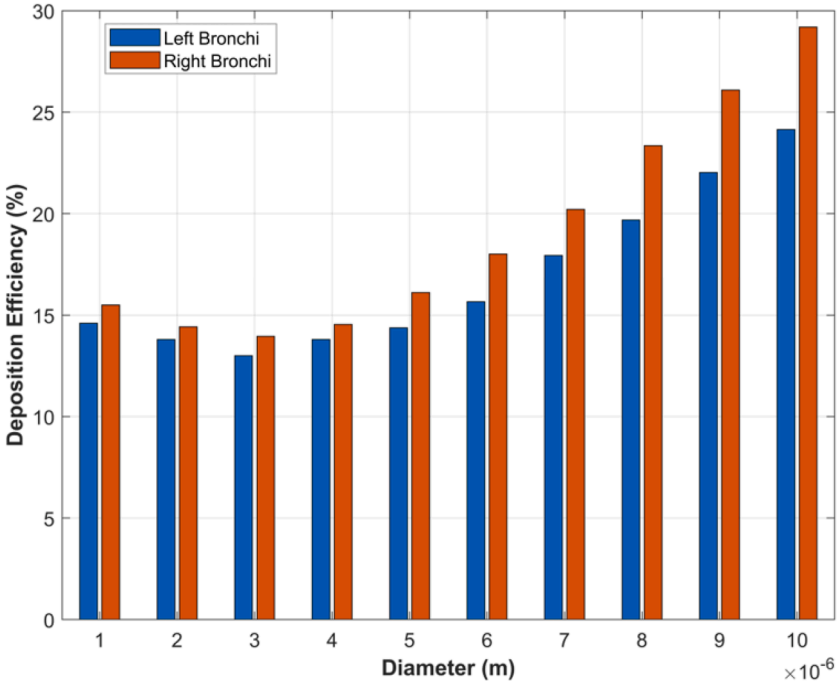

Fig. 16. Deposition of microplastic particles for varying size in the left and right lung bronchi at 40 LPM.

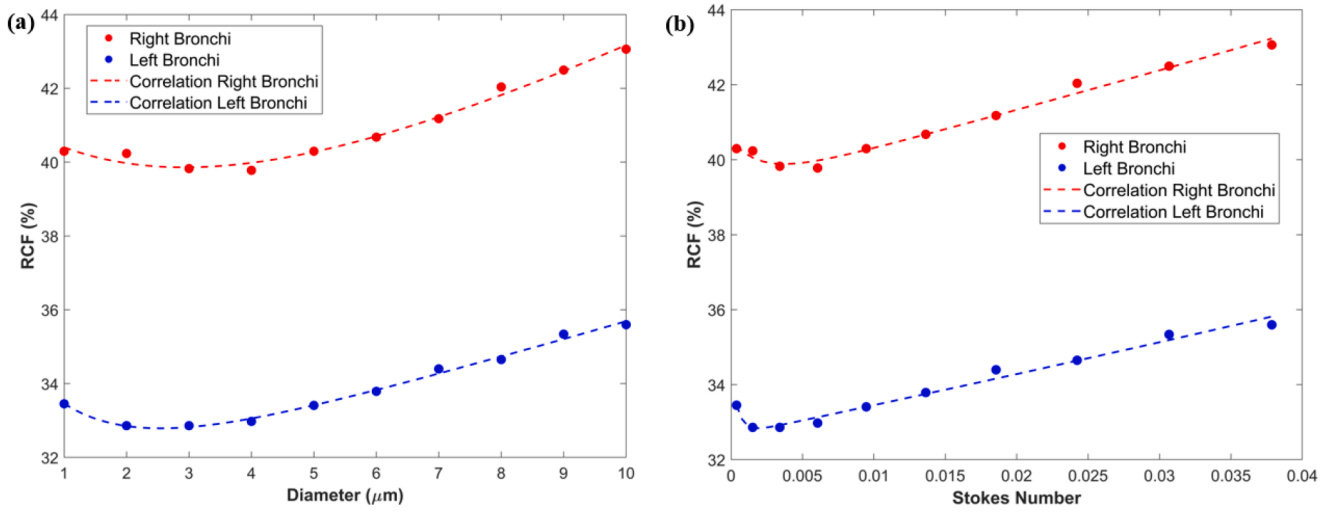

Fig. 17. Risk contribution fraction of microplastic inhalation in left and right bronchi at 40 LPM for varying (a): particle diameter; and (b): Stokes number.

the lung airway, fluid density, viscosity, speed, and microplastic particle size. The Stokes number indicates the likelihood of inhaled microplastic particles being deposited in the lung airways by quantifying the balance between inertial and viscous forces acting on the particles as they move through the airflow. Fig. 17(b) shows a higher risk contribution fraction of microplastic inhalation at large Stokes number. The fitted empirical equations for the RCF of microplastic inhalation in the right and left bronchi of lungs against the microplastic particle diameter (d_p) and Stokes number (Skt) are:

$$RCF_{RB} = 5.51.\exp\left(-0.33 \times d_p\right) \tag{13}$$

$$RCF_{LB} = 4.21.\exp\left(-0.80 \times d_p\right) \tag{14}$$

$$RCF_{RB} = 1.23.\exp(-472.15 \times Skt) \tag{15}$$

$$RCF_{LB} = 1.59.\exp(-1894.26 \times Skt) \tag{16}$$

For a detailed understanding of microplastic deposition in the tracheobronchial airways, concentration plots of deposited microplastic particles for different particle diameter ranges along the vertical length of the lung model are shown in Fig. 18. Normalized count, defined as the ratio of the number of particles deposited in a range to the number of unique particle diameters in that range, is used to account for uneven particle size ranges. At the lower flow rate of 7.5 LPM, the large particles with size 8–10 μm are deposited more in the airways, especially during inhalation, followed by the size range of 4–7 μm. The smaller particles with sizes 1–3 μm mostly follow the airflow streamlines due to reduced Stokes number and inertial impaction and escape to deposit beyond G15. During exhalation, the trend is somewhat similar with smaller particles depositing less and size ranges of 4-7 μm and 8-10 μm depositing more, especially in the main bronchi ($-0.05\ m > y > -0.08\ m$).

Fig. 19 shows the deposited microplastic concentration plots for other inhalation flow rates. For a lower flow rate of 7.5 LPM, despite

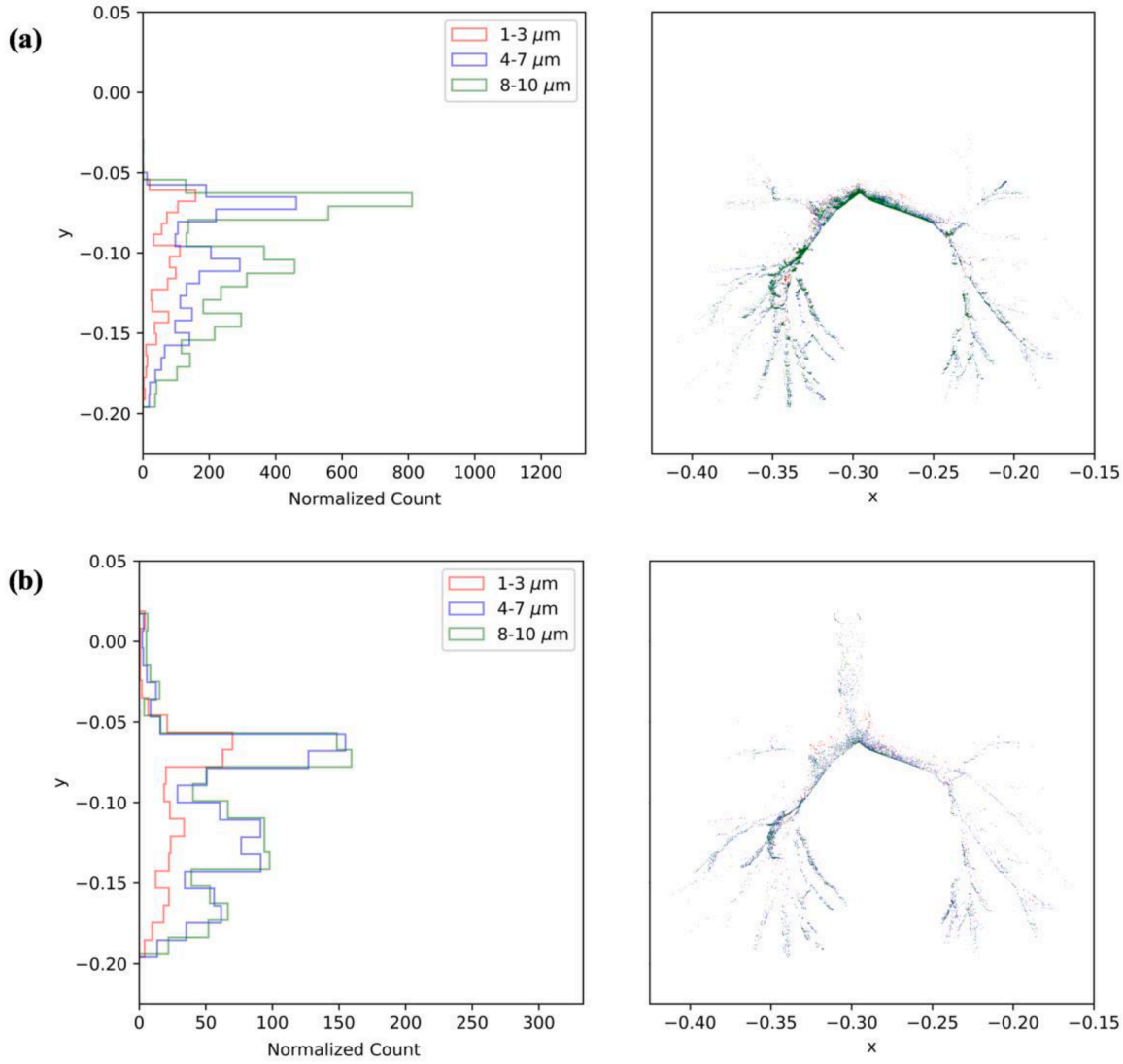

Fig. 18. Deposited microplastic particles count and visualization plot along the tracheobronchial airways for different particle sizes at the inhalation flow rate of 7.5 LPM and 0.25 Hz frequency for (a): inhalation; and (b): exhalation.

having almost similar deposition hotspot sites, the deposited microplastic particle count for the breathing frequency of 0.5 Hz is lower than 0.25 Hz during inhalation. This is due to the longer inhalation period of 0.25 Hz which gives particles more time to be trapped in the airway walls. The breathing cycle with higher frequency has more microplastic deposition during exhalation as compared the exhalation phase of lower cycle frequency. The availability of more microplastic particles in fluid during inhalation in the case of 0.5 Hz frequency promotes their deposition during the exhalation phase. For larger flow rates of 15 LPM and 40 LPM, the deposited microplastic concentrations are higher. The deposition hotspots as well as particle count for larger sizes in case of 15 LPM flow rate and 0.5 Hz frequency (Fig. 19) are approximately similar to the 7.5 LPM flow rate and 0.25 Hz frequency (Fig. 18). This signifies the role of the breathing cycle period on the deposition of microplastic particles in the lung airways. The only reason for a relatively higher overall deposition at a 15 LPM flow rate is the increase in the penetration of small size microplastics (1–3 μm) which were depositing very less in the case of 7.5 LPM. At the 40 LPM flow rate, the particle count for all three size ranges has become almost equal. Small size microplastics (1–3 μm) deposit slightly higher in the main bronchi region during inhalation at 40 LPM flow rate. At this flow rate, the high Stokes number along with inertial impaction hinders the inhaled microplastic particles from accurately navigating the flow streamlines and they deposit due to sudden path changes and flow separations.

Figs. 20 and 21 illustrates the trends of different microplastic shapes that deposit in the tracheobronchial airways at different inhalation flow rates. There is no consistent pattern in the number of deposited particles for any specific microplastic shape. Instead, all four shapes tend to deposit in similar hotspot regions, with the number of maximum deposited particles varying between shapes at each hotspot site. For lower flow rates, each peak in the histogram plot represents the airway bifurcation where the majority of the microplastics tend to deposit. For a larger flow rate, the microplastic deposition dominates in the bifurcation and airway regions of main bronchi up to G8 approximately ($-0.05\ m > y > -0.15\ m$) and beyond G8 ($y < -0.15\ m$), the deposition starts to decrease with only a minimal particle trapping in the central airways. The slight differences between the deposited particles in the airways between different shapes are subjective to factors including varying drag and inertial force specific to each particle shape and aerodynamic efficiency of different particle geometries.

Fig. 22 provides an overview of the deposited concentration of microplastic particles for different inhalation flow rates. The maximum deposition of microplastics is found at a larger flow rate during inhalation. While, during the exhalation, the smaller flow rate dominates the

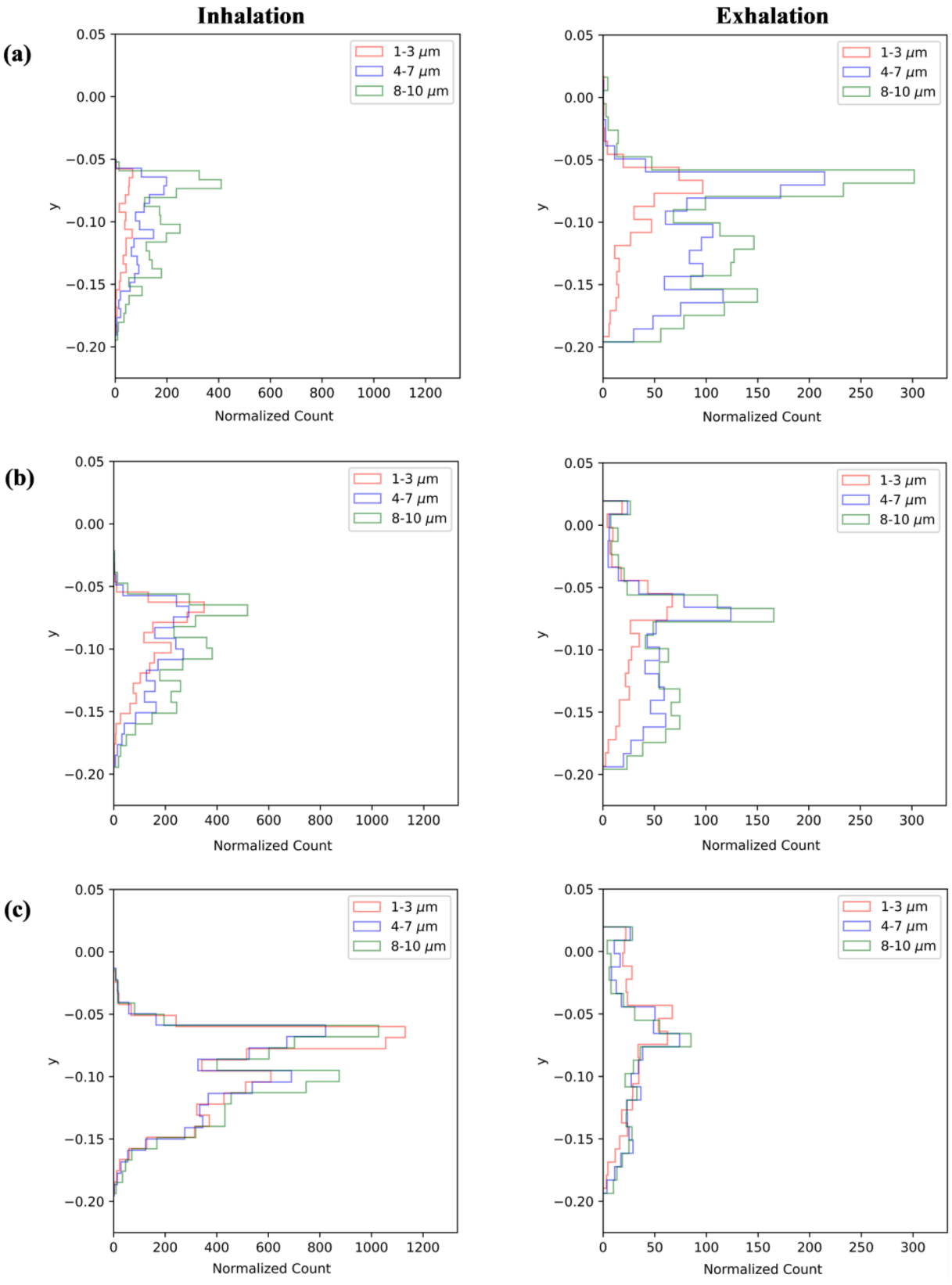

Fig. 19. Deposited microplastic particles count plots along the tracheobronchial airways for different particle sizes at the breathing cycle frequency of 0.5 Hz and inhalation flow rate of (a): 7.5 LPM, (b): 15 LPM, and (c) 40 LPM.

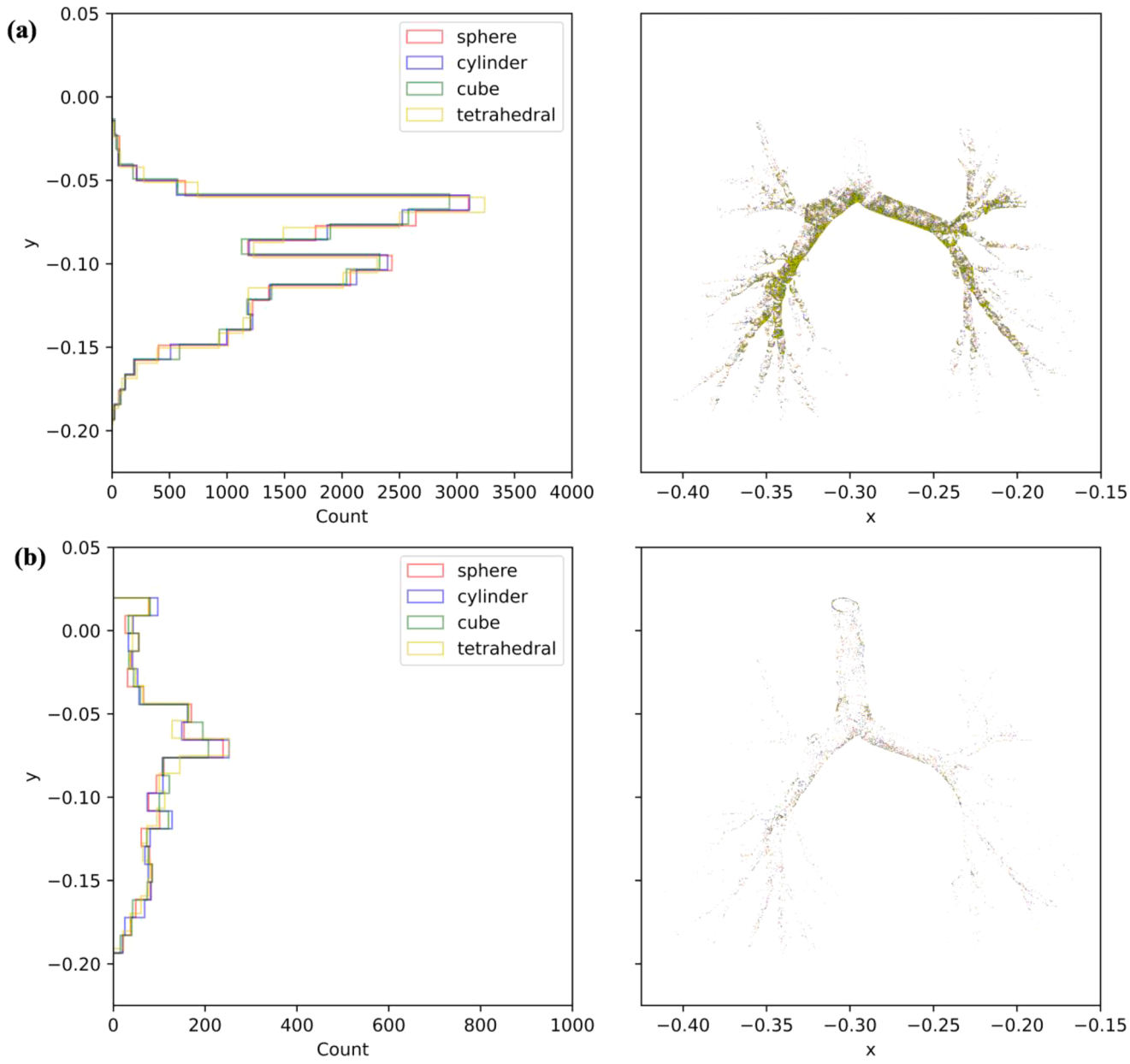

Fig. 20. Deposited microplastic particles count and visualization plot along the tracheobronchial airways for different particle shapes at the inhalation flow rate of 40 LPM and 0.5 Hz frequency for (a): inhalation; and (b): exhalation.

microplastic deposition in the tracheobronchial airways. During high-flow inhalation, the incoming air at high velocities creates turbulent flow as it navigates through the branching airways. This turbulence enhances the likelihood of particle deposition due to increased inertial impaction against the airway walls. Whereas during high-flow exhalation, the air is expelled more smoothly because the exiting flow tends to be more streamlined and less turbulent compared to the chaotic incoming air. This reduced turbulence during exhalation decreases the chance of particles being trapped in the airways, leading to lower particle deposition. At low flow rates during exhalation, the air moves more slowly and smoothly through the airways, which can reduce turbulence and cause particles to remain in the airways for a longer time. This extended residence time increases the likelihood of particles being deposited easily and more in the initial generations, especially the large particle.

5. Conclusions

Recent research has uncovered the alarming presence of microplastic particles in human lung tissues, marking a significant need for understanding their impact on respiratory health. Continuous inhalation of such pollutants has been found to interfere with the normal functioning of the lungs and leading to several respiratory disorders. This highlights the urgent need to address the widespread microplastic contamination affecting individuals globally. The transport and accumulation of microplastics in the lungs need further investigation to fully describe the implications concerning human health. The current study investigated the impact of varying inhalation patterns and inhaled microplastic particle sizes on their penetration in the lung airways. The analysis of the deposition patterns and flow dynamics within different airway regions enhanced the understanding of microplastic behavior in the respiratory system, which is essential for health assessments. The conclusions are summarized below.

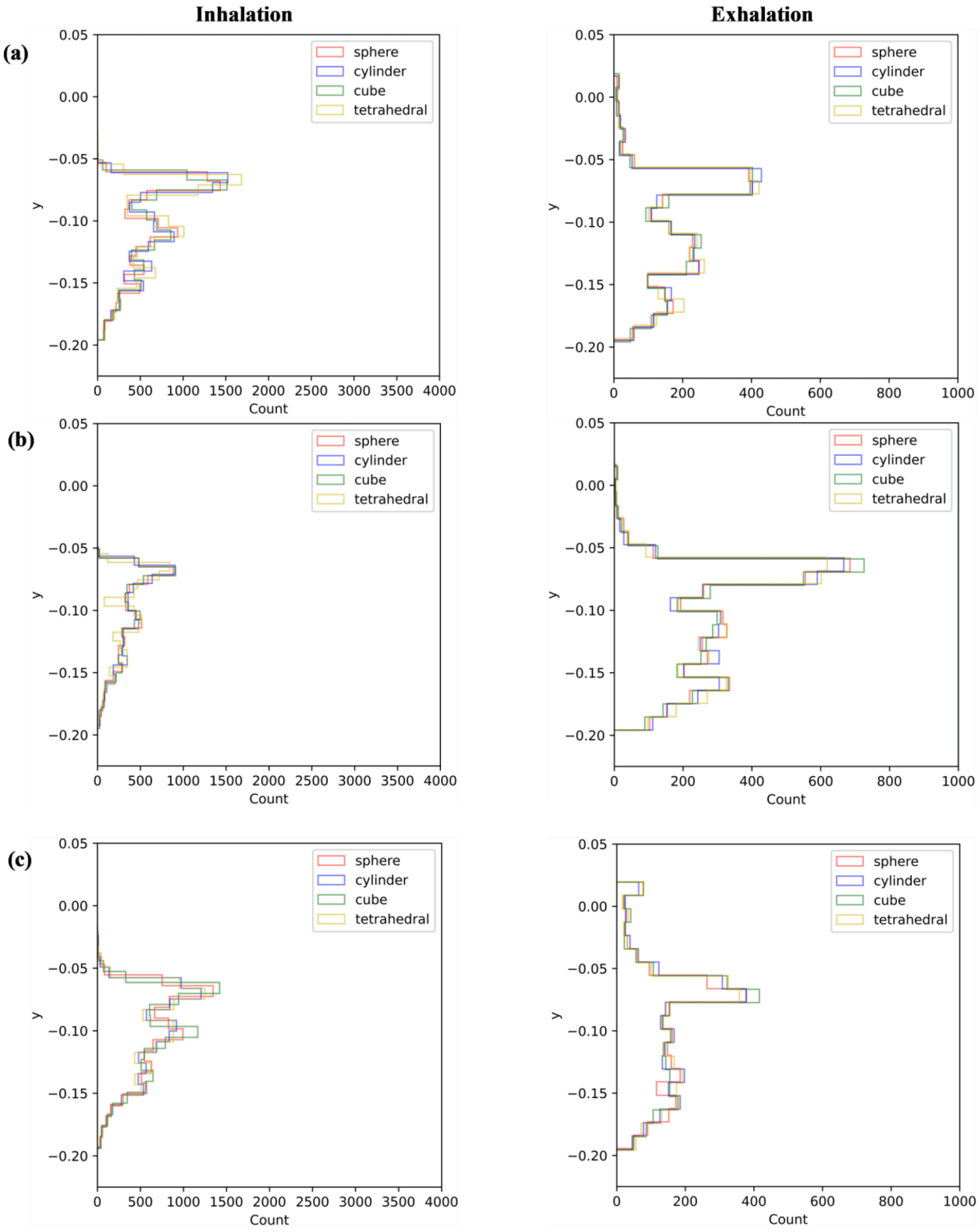

Fig. 21. Deposited microplastic particles count plots along the tracheobronchial airways for different particle shapes at the inhalation flow rate of (a): 7.5 LPM, 0.25 Hz; (b): 7.5 LPM, 0.5 Hz; and (c) 15 LPM, 0.5 Hz.

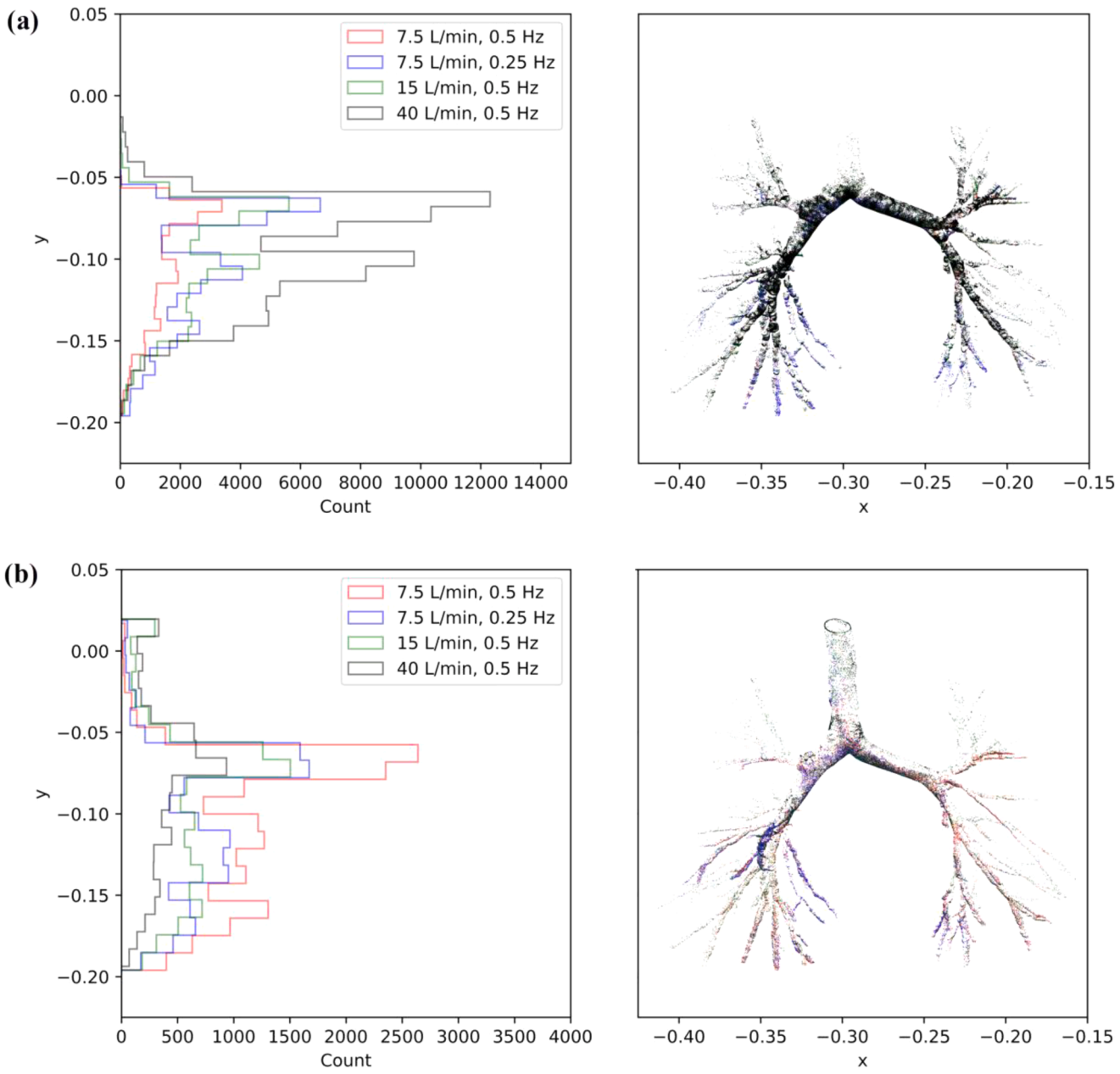

Fig. 22. Total deposited microplastic particles along the tracheobronchial airways for different inhalation flow rates during (a): inhalation; and (b): exhalation.

- Both a decrease in flow rate and an increase in cycle frequency led to an overall reduced deposition efficiency. The minimal microplastic deposition is found at the small flow rate of 7.5 LPM with a cycle frequency of 0.5 Hz. A further decrease in this frequency to 0.25 Hz causes a significant increase in the microplastic penetration in the left and right bronchi.
- The high airflow volume in the right bronchi leads to higher microplastic deposition in almost all the right generations of the tracheobronchial airways than left generations. LPM The majority of microplastic deposition occurs during the inhalation phase. At a flow rate of 40 LPM, the total deposition efficiency in the right bronchi during inhalation is 9.7 times higher than during exhalation. Likewise, in the left bronchi, the total microplastic deposition during inhalation is 9 times greater than during exhalation.
- Deposition in the early generations (G1-G8) increases with higher flow rates, while deposition in the lower generations (G9-G15) decreases. For example, at a flow rate of 40 LPM, the deposition rate in G1-G8 is 15.9 % higher than at 15 LPM. In contrast, the deposition rate in G9 to G15 at 40 LPM is 0.6 % lower than at 15 LPM.
- The calculated risk contribution fraction of microplastic inhalation for the right bronchi is 20.8 % higher than left bronchi of the lung. This risk fraction directly depends upon the inhaled microplastic size and Stokes number.
- At small flow rates, the microplastic particle size in the range of 4–10 μm deposits more in the main bronchus. The particles with sizes 1–3 μm have higher deposition at a large inhalation flow rate. Furthermore, the deposition hotspots of inhaled microplastics during inhalation are the main bronchi and initial airways up to G8. These deposition hotspots shift to the left and right main bronchus during the exhalation.

The findings of the current study on the microplastic flow and deposition in the lung airways could facilitate the health risk assessments under severe pollutant particle inhalation. The limitations of the

current study include the assumption of rigid airway wall interactions, the use of a sinusoidal velocity profile, and the reliance on an incomplete respiratory model. Future studies would focus on the more accurate prediction of the flow of microplastics with various geometric and nongeometric particle shapes in complete lung model by developing in-house discrete element method codes and numerical models.

Ethics statement

This study was approved by the Prince Charles Hospital Human Research Ethics Committee (Approval No. HREC/16/QPCH/276) and the Queensland University of Technology Human Research Committee (Approval No. 1600000923).

CRediT authorship contribution statement

Hafiz Hamza Riaz: Writing – original draft, Visualization, Validation, Investigation, Formal analysis, Data curation. **Abdul Haseeb Lodhi:** Writing – review & editing, Visualization, Validation, Investigation, Formal analysis, Data curation. **Adnan Munir:** Writing – review & editing, Supervision, Conceptualization. **Ming Zhao:** Writing – review & editing. **Muhammad Hamza Ali:** Writing – review & editing, Formal analysis, Data curation. **Emilie Sauret:** Writing – review & editing. **YuanTong Gu:** Writing – review & editing. **Mohammad S. Islam:** Writing – review & editing, Supervision, Conceptualization.

Declaration of competing interest

The authors declare that they have no known competing financial interests or personal relationships that could have appeared to influence the work reported in this paper.

Data availability

Data will be made available on request.

References

Amato-Lourenço, L.F., Carvalho-Oliveira, R., Júnior, G.R., Dos Santos Galvão, L., Ando, R.A., Mauad, T., 2021. Presence of airborne microplastics in human lung tissue. J. Hazard. Mater. 416, 126124.

Arsalanloo, A., Abbasalizadeh, M., Khalilian, M., Saniee, Y., Ramezanpour, A., Islam, M. S., 2022. A computational approach to understand the breathing dynamics and pharmaceutical aerosol transport in a realistic airways. Adv. Powder Technol. 33, 103635.

Bowes Iii, S.M., Swift, D.L., 1989. Deposition of inhaled particles in the oral airway during oronasal breathing. Aerosol Sci. Technol. 11, 157–167.

Chan, T.L., Lippmann, M., 1980. Experimental measurements and empirical modelling of the regional deposition of inhaled particles in humans. Am. Ind. Hyg. Assoc. J. 41, 399–409.

Chen, X., Feng, Y., Zhong, W., Sun, B., Tao, F., 2018. Numerical investigation of particle deposition in a triple bifurcation airway due to gravitational sedimentation and inertial impaction. Powder. Technol. 323, 284–293.

Cheng, Y.-S., Zhou, Y., Chen, B.T., 1999. Particle deposition in a cast of human oral airways. Aerosol Sci. Technol. 31, 286–300.

Chithra, V., Nagendra, S.S., 2013. Chemical and morphological characteristics of indoor and outdoor particulate matter in an urban environment. Atmos. Environ. 77, 579–587.

Chong, K.L., Ng, C.S., Hori, N., Yang, R., Verzicco, R., Lohse, D., 2021. Extended lifetime of respiratory droplets in a turbulent vapor puff and its implications on airborne disease transmission. Phys. Rev. Lett. 126, 034502.

Ciloglu, D., 2020. A numerical study of the aerosol behavior in intra-acinar region of a human lung. Phys. Fluids 32.

Do-Quang, M., Amberg, G., Brethouwer, G., Johansson, A.V., 2014. Simulation of finite-size fibers in turbulent channel flows. Phys. Rev. E 89, 013006.

Geyer, R., Jambeck, J.R., Law, K.L., 2017. Production, use, and fate of all plastics ever made. Sci. Adv. 3, e1700782.

Gou, D., Zhu, Q., Chan, H.-K., Kourmatzis, A., Cheng, S., Yang, R., 2024. Effects of the deformation and size of the upper airway on the deposition of aerosols. Int. J. Pharm. 657, 124165.

Gupta, J.K., Lin, C.H., Chen, Q., 2010. Characterizing exhaled airflow from breathing and talking. Indoor. Air. 20, 31–39.

Haghnegahdar, A., Zhao, J., Feng, Y., 2019. Lung aerosol dynamics of airborne influenza A virus-laden droplets and the resultant immune system responses: an in silico study. J. Aerosol. Sci. 134, 34–55.

Haider, A., Levenspiel, O., 1989. Drag coefficient and terminal velocity of spherical and nonspherical particles. Powder. Technol. 58, 63–70.

Heyder, J., 2004. Deposition of inhaled particles in the human respiratory tract and consequences for regional targeting in respiratory drug delivery. Proc. Am. Thorac. Soc. 1, 315–320.

Huang, S., Huang, X., Bi, R., Guo, Q., Yu, X., Zeng, Q., Huang, Z., Liu, T., Wu, H., Chen, Y., 2022. Detection and analysis of microplastics in human sputum. Environ. Sci. Technol. 56, 2476–2486.

Huang, X., Saha, S.C., Saha, G., Francis, I., Luo, Z., 2024. Transport and deposition of microplastics and nanoplastics in the human respiratory tract. Environ. Adv. 16, 100525.

Inoue, M., Homma, T., Aoki, H., Sumi, M., Ohtsu, I., Tomioka, S., Hagiya, M., Yamashita, Y., Hasegawa, S., 1997. Effect of respiratory rate on respiratory patterns in patients with chronic obstructive pulmonary disease. Internal Med. 36, 771–775.

Inthavong, K., Choi, L.-T., Tu, J., Ding, S., Thien, F., 2010. Micron particle deposition in a tracheobronchial airway model under different breathing conditions. Med. Eng. Phys. 32, 1198–1212.

Islam, M.S., Larpruenrudee, P., Paul, A.R., Paul, G., Gemci, T., Gu, Y., Saha, S.C., 2021. SARS CoV-2 aerosol: How far it can travel to the lower airways? Phys. Fluids 33.

Islam, M.S., Rahman, M.M., Larpruenrudee, P., Arsalanloo, A., Beni, H.M., Islam, M.A., Gu, Y., Sauret, E., 2023. How microplastics are transported and deposited in realistic upper airways? Phys. Fluids 35.

Jenner, L.C., Rotchell, J.M., Bennett, R.T., Cowen, M., Tentzeris, V., Sadofsky, L.R., 2022. Detection of microplastics in human lung tissue using μFTIR spectroscopy. Sci. Total Environ. 831, 154907.

Jia, L., Zhang, L., Yu, S., 2018. Deposition of non-spherical microparticles in the human upper respiratory tract. Particuology 36, 185–189.

Jing, H., Ge, H., Wang, L., Choi, S., Farnoud, A., An, Z., Lai, W., Cui, X., 2023. Investigating unsteady airflow characteristics in the human upper airway based on the clinical inspiration data. Phys. Fluids 35.

Khoa, N.D., Li, S., Phuong, N.L., Kuga, K., Yabuuchi, H., Kan-O, K., Matsumoto, K., Ito, K., 2023. Computational fluid-particle dynamics modeling of ultrafine to coarse particles deposition in the human respiratory system, down to the terminal bronchiole. Comput. Methods Programs Biomed. 237, 107589.

Kleinstreuer, C., Zhang, Z., Li, Z., Roberts, W.L., Rojas, C., 2008. A new methodology for targeting drug-aerosols in the human respiratory system. Int. J. Heat. Mass Transf. 51, 5578–5589.

Lippmann, M., Albert, R.E., 1969. The effect of particle size on the regional deposition of inhaled aerosols in the human respiratory tract. Am. Ind. Hyg. Assoc. J. 30, 257–275.

Marchioli, C., Fantoni, M., Soldati, A., 2010. Orientation, distribution, and deposition of elongated, inertial fibers in turbulent channel flow. Phys. Fluids 22.

Marcus, G.G., Parsa, S., Kramel, S., Ni, R., Voth, G.A., 2014. Measurements of the solid-body rotation of anisotropic particles in 3D turbulence. New. J. Phys. 16, 102001.

Rahman, M., Zhao, M., Islam, M.S., Dong, K., Saha, S.C., 2022. Numerical study of nano and micro pollutant particle transport and deposition in realistic human lung airways. Powder. Technol. 402, 117364.

Rahman, M.M., Zhao, M., Islam, M.S., Dong, K., Saha, S.C., 2021a. Aging effects on airflow distribution and micron-particle transport and deposition in a human lung using CFD-DPM approach. Adv. Powder Technol. 32, 3506–3516.

Rahman, M.M., Zhao, M., Islam, M.S., Dong, K., Saha, S.C., 2021b. Numerical study of nanoscale and microscale particle transport in realistic lung models with and without stenosis. Int. J. Multiphase Flow 145, 103842.

Rahman, M.M., Zhao, M., Islam, M.S., Dong, K., Saha, S.C., 2024. A numerical study on sedimentation effect of dust, smoke and traffic particle deposition in a realistic human lung. Int. J. Multiphase Flow 171, 104685.

Riaz, H.H., Lodhi, A.H., Munir, A., Zhao, M., Farooq, U., Qadri, M., Islam, M.S., 2024. Breathing in danger: mapping microplastic migration in the human respiratory system. Phys. Fluids 36.

Soldati, A., Marchioli, C., 2009. Physics and modelling of turbulent particle deposition and entrainment: review of a systematic study. Int. J. Multiphase Flow 35, 827–839.

Stahlhofen, W., Gebhart, J., Heyder, J., 1980. Experimental determination of the regional deposition of aerosol particles in the human respiratory tract. Am. Ind. Hyg. Assoc. J. 41, 385–398a.

Tanprasert, S., Kampeewichean, C., Shiratori, S., Piemjaiswang, R., Chalermsinsuwan, B., 2023. Non-spherical drug particle deposition in human airway using computational fluid dynamics and discrete element method. Int. J. Pharm. 639, 122979.

Vethaak, A.D., Legler, J., 2021. Microplastics and human health. Science (1979) 371, 672–674.

Voth, G.A., Soldati, A., 2017. Anisotropic particles in turbulence. Annu Rev. Fluid. Mech. 49, 249–276.

Wadell, H., 1934. The coefficient of resistance as a function of Reynolds number for solids of various shapes. J. Franklin. Inst. 217, 459–490.

Wang, J., Alipour, M., Soligo, G., Roccon, A., De Paoli, M., Picano, F., Soldati, A., 2021. Short-range exposure to airborne virus transmission and current guidelines. Proc. Natl Acad. Sci. 118, e2105279118.

Xu, C., Zhang, B., Gu, C., Shen, C., Yin, S., Aamir, M., Li, F., 2020. Are we underestimating the sources of microplastic pollution in terrestrial environment? J. Hazard. Mater. 400, 123228.

Xu, M., Halimu, G., Zhang, Q., Song, Y., Fu, X., Li, Y., Li, Y., Zhang, H., 2019. Internalization and toxicity: a preliminary study of effects of nanoplastic particles on human lung epithelial cell. Sci. Total Environ. 694, 133794.

Ya, H., Jiang, B., Xing, Y., Zhang, T., Lv, M., Wang, X., 2021. Recent advances on ecological effects of microplastics on soil environment. Sci. Total Environ. 798, 149338.

Yang, Z., Wang, M., Feng, Z., Wang, Z., Lv, M., Chang, J., Chen, L., Wang, C., 2023. Human microplastics exposure and potential health risks to target organs by different routes: a review. Curr. Pollut. Rep. 9, 468–485.

Zuo, Y.Y., Uspal, W.E., Wei, T., 2020. Airborne transmission of COVID-19: aerosol dispersion, lung deposition, and virus-receptor interactions. ACS. Nano 14, 16502–16524.